Microwave Assisted Synthesis of Silver Nanorods

by

Srichandana Nandikonda

A thesis submitted to the Graduate Faculty of
Auburn University
in partial fulfillment of the
requirements for the Degree of
Polymer and Fiber Engineering, Master of Science

Auburn, Alabama
August 9, 2010

Keywords: Silver nanorods, Microwave synthesis, Continuous Flow Synthesis

Approved by

Edward W. Davis, Chair, Assistant Research Professor of Polymer and Fiber Engineering
Maria L. Auad, Assistant Professor of Polymer and Fiber Engineering
Gisela Buschle-Diller, Professor of Polymer and Fiber Engineering

Abstract

Silver nanoparticles have unique and distinctive properties like optical, electrical and conductive properties. These properties of nanoparticles depend on their size, shape and crystalinity. There has been a lot of work published on synthesis of silver nanoparticles with controlled morphology. However, there has not been much work done on silver nanoparticles with controlled morphology, high yield and less reaction times.

The aim of this research is to synthesize silver nanowires with high yield at low reaction timings. In order to achieve this, different salts like NaCl, KCl, $MgCl_2$, $CaCl_2$, $MnCl_2$, $CuCl_2$ and $FeCl_3$ where used. The effect of salt on the silver nanowires is evaluated by using SEM images. In addition , effect of concentration of salt on yield of silver nanowires and a novel method for the continuous flow synthesis of silver nanoparticles have been studied. Characterization of silver nanoparticles has been done using SEM, TEM and optical microscopy.

Acknowledgments

The author would like to express her thanks and gratitude to her advisor Dr. Edward W. Davis, for his guidance, support and invaluable suggestions. The author also expresses her gratitude to the other members of her advisory committee, Dr. Maria L. Auad and Dr. Gisela Buschle-Diller, for their constructive criticism and advice. Thanks to Dr. Xinyu Zhang for all his assistance and suggestions. Thanks to the Department of Polymer and Fiber Engineering for providing financial support. Thanks to all faculty, staff and colleagues of the Department of Polymer and Fiber engineering for being supportive and for providing welcoming environment.

Many thanks to my father, my extended family, my sister and sister in-law for being a part of my life, and providing encouragement and support throughout the years; I am truly grateful to my late mother without whom, education in my life would not have been possible.

Table of Contents

List of Tables

List of Figures

List of Abbreviations

Ag^0	Silver atom
Ag^+	Silver ion
1D	one dimensional
NaCl	Sodium Chloride
KCl	Potassium Chloride
$MgCl_2$	Magnesium Chloride
$CaCl_2$	Calcium Chloride
$MnCl_2$	Manganese Chloride
$CuCl_2$	Copper Chloride
$FeCl_3$	Ferric Chloride

CHAPTER 1

Introduction

1.1 Introduction:

Silver nanoparticles have many applications like in chemical, biological and optical sensors.[1] Silver nanoparticles exhibit a high efficiency of plasmon excitation compared to Au and Cu.[2] Silver 1D nanostructures like silver nanorods and silver nanowires have gained a lot of attention due to their unique properties and applications. For example, SERS (Surface Enhanced Raman Scattering) and silver nanorods quickly reveal the viral structures.[3] Figure 1.1 shows the illustration of silver nanorod arrays and SERS to rapidly to detect human viruses in specimen volumes. Also it can differentiate between respiratory viruses, virus strains, and virus containing gene deletions without manipulating the virus. SERS is known for its high sensitivity due to its surface plasmon effects lacks behind at uniform substrate formation. A substrate was formed by placing rows of silver nanorods at a density of 13 nanorods/mm^2 and a 72°±4° angle from the normal on the substrate that holds the sample. This substrate has enhanced the degree of sensitivity and specificity for rapid detection of trace levels of viruses.

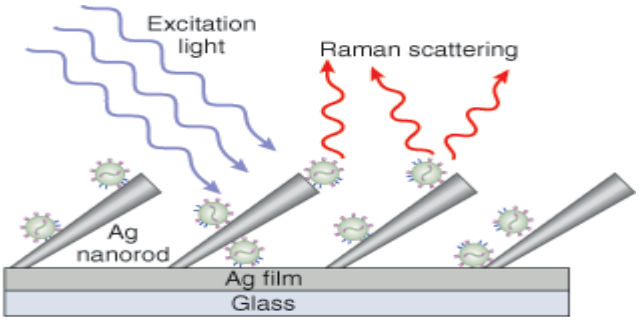

Figure 1.1: Ag nanorod arrays and SERS for rapid detection of human viruses[3]

Polymer/metal nanocomposite containing anisotropic metal nanostructures such as metal nanorods and nanowires appeared extremely more sensitive and responsive to mechanical stimuli than nanocomposites containing spherical nanoparticles. Figure 1.2 shows the schematic of the nanocomposite formed by silver nanorods in Poly vinyl alcohol matrix.[4] After uniaxial stretching of the supporting polymer matrix, the elongated silver nanorods assume the direction of the drawing. This results in a yielding material with a strong dichroic response of the absorption behavior. The film changes its color when observed under linearly polarized light already at moderate drawings. These nanocomposite films have potential in applications such as color polarizing filters, radiation responsive polymeric objects and smart flexible films in packaging applications.

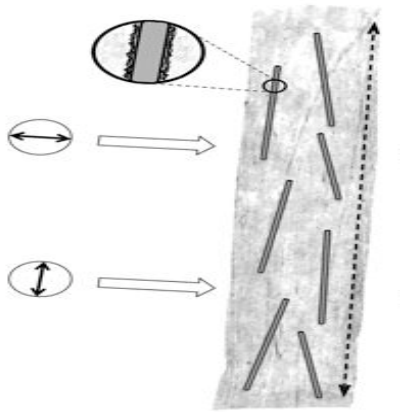

Figure 1.2: PVA and silver nanorod composite[4]

Application of silver nanowires in low cost paper batteries is one of the recent developments as shown in figure 1.3.[5] By dipping an ordinary piece of paper into ink infused with carbon nanotubes and silver nanowires, scientists have been able to create a low-cost battery or super capacitor that is ultra-lightweight, bendable and very durable. The paper can be crumpled, folded or even soaked in acidic or basic solutions and still will work. Coating a sheet of paper with ink made of carbon nanotubes and silver nanowires produced a highly conductive

storage device that could be used in a multitude of applications. The flexibility of paper allows for many clever applications. One of the applications is in LEDS (light-emitting diode).

Figure 1.3: Paper coated with ink made of carbon nanotubes and silver nanowires.[5]

All these unique applications are achieved due to the anisotropic properties of silver nanorods and wires. Synthesis plays a major role for all these applications as aspect ratio and uniformity plays a major role. In order to explore the key parameters for the synthesis of silver nanorods, five different topics have been considered. Those are effect of shape of the container on synthesis of silver nanorods, continuous flow synthesis of silver nanorods, effect of alkali and alkaline earth metals, effect of transition metals, and effect of missing methods on synthesis of silver nanorods.

Chapter 2

Literature Review

2.1 Nanotechnology

Materials in which characteristic size scale is on the order of 1 nm are called nanomaterials. The application of these materials computing[6], sensors[7] biomedical[8] and other areas has attracted considerable interest in the last two decades. However, nanotechnology has been used since the early 16th century Damascus swords and other. The modern concept of nanotechnology was first described by physicist Richard P. Feynman in his 1959 lecture "There's plenty of room at the bottom." Nanotechnology or Nanoscience has been defined as “concerned with materials and systems whose structure and components exhibit novel and significantly improved physical, chemical and biological properties, phenomena and process due to their nanoscale size”.

A nanometer is one billionth of a meter (10^{-9} m). Nanoparticles have characteristic physical, chemical, electronic, electrical, mechanical, magnetic, thermal, dielectric, optical and biological properties.[9,10] Decreasing the dimension of nanoparticles has pronounced effect on the physical properties that significantly differ from the bulk material. These physical properties are caused by their large surface atom, large surface energy, spatial confinement and reduced imperfections. Nanoparticles have advantages over bulk materials due to their surface plasmon resonance (SPR), enhanced Rayleigh scattering and surface enhanced Raman scattering (SERS) in metal nanoparticles, quantum size effect in semiconductors and super magnetism in magnetic

materials. Therefore, nanoparticles are considered as building blocks of the next generation of optoelectronics, electronics, and various chemical and biochemical sensors.[11,12]

Nanotechnology has been developed through two areas. Those are development of synthesis techniques and development of characterization technique. In case of synthesis techniques, Michael Faraday first reported the synthesis and optical properties of (colloidal) gold nanoparticles in 1857.[13] Nanoparticles can be synthesized mainly in 2 different approaches, Bottom-up and Top-down[14]. Colloidal dispersion is a good example of Bottom-up method where atoms or molecules are condensed to form nanoparticles. Milling and attrition is the typical Top down methods, where a solid material is finely divided to nanoscale to form nanoparticles. Due to the ability to control size and shape the bottom up approach is preferred. However, top down synthesis methods are not available to produce all shapes and geometries of interest.

In the case of characterization techniques, structural and chemical characterization techniques have got major developments. Mie's theory is of great interest of this day because of its application to nanoparticles, but has faced many challenges in case of anisotropic structures like cubes, triangles, rods.[15] Mie's theory has given an exact solution to Maxwell's equation, where the absorption and scattering spectra of spherical particles has been described.

Structural characterization can be done using X-ray diffraction (XRD), Scanning electron microscopy (SEM) and Transmission electron microscopy (TEM). XRD is used for determining crystalinity, crystal structures and lattice constants of nanoparticles[16]. SEM is the most widely used characterization technique for nanomaterials and structures.[17] SEM can operate magnifications from 10 to 300k and also it gives chemical composition information near surface. Field emission scanning electron microscopy (FESEM) is advanced SEM, where clearer and less electro statically distorted images can be obtained[18]. High quality, low voltage images are

obtained with negligible electro charging of samples. TEM gives higher magnification from 50 to 10^6 and it gives both image and diffraction information[19]. Scanning probe microscopy (SPM) is relatively new characterization technique and it provides 3D (3 dimensional) real space images[20]. SPM has 2 major members scanning tunneling microscopy (STM) and atomic force microscopy (AFM). STM requires electrically conductive samples, where as AFM can be operated on any sample[21,22]. STM and AFM can provide topographic images and almost all solid surfaces can be studied in air, vacuum or liquid. STM was first developed by Binning in 1981 and AFM was invented a bit later.

Chemical characterization can be done using optical, electron and ionic spectroscopy to determine the surface and interior atoms and compounds as well as their spatial distributions. Optical microscopy is used to determine the electronic structures of atoms, ions, molecules and crystals. Optical spectroscopy includes absorption and transmission spectroscopy, photoluminescence, infrared and raman spectroscopy. Electron spectroscopy includes Energy dispersive X-ray spectroscopy (EDS)[23], auger electron spectroscopy (AES)[24] and X-ray photoelectron spectroscopy (XPS)[25]. Electron spectroscopy is used to determine chemical composition by the X-rays and auger electrons emitted by a material.

2.1.1 Nanomaterials:

There are several classification schemes for the plethora of nanoparticles currently reported in the literature. These schemes can be based on shape or materials. Nanomaterials in general can be classified by the material, shape, or mode of use (composite, individual particles, etc.). Based on material type Nanomaterials are broadly classified as organic or inorganic. Organic nanomaterials include carbon nanotubes, and nanosized polymer particles. Inorganic nanomaterials include ceramic particles or metal oxides, and pure metal nanoparticles.

2.1.1.1 Organic nanomaterials

Organic nanomaterials are the compounds containing carbon, like carbon nanotubes and nanosized polymer materials. Organic nanomaterials are well known for their optoelectronic properties[26], good doping properties[27], high reaction activity[28], good processability[29], and high photoluminescence (PL) efficiency[30], which make them complementary to the inorganic materials.

Organic nanomaterials have been synthesized using different methods like reprecepitation[31], evaporation, and microemulsion[32], and laser irradiation[33]. These materials have been fabricated in different shapes like nanoparticles[34], nanoplatelets[35], nanoribbons, nanowires, nanotubes,[36] nanovesicles[37], and nanobelts[38]. Figure 2.1 shows the different structures formed with different molecular design[39].

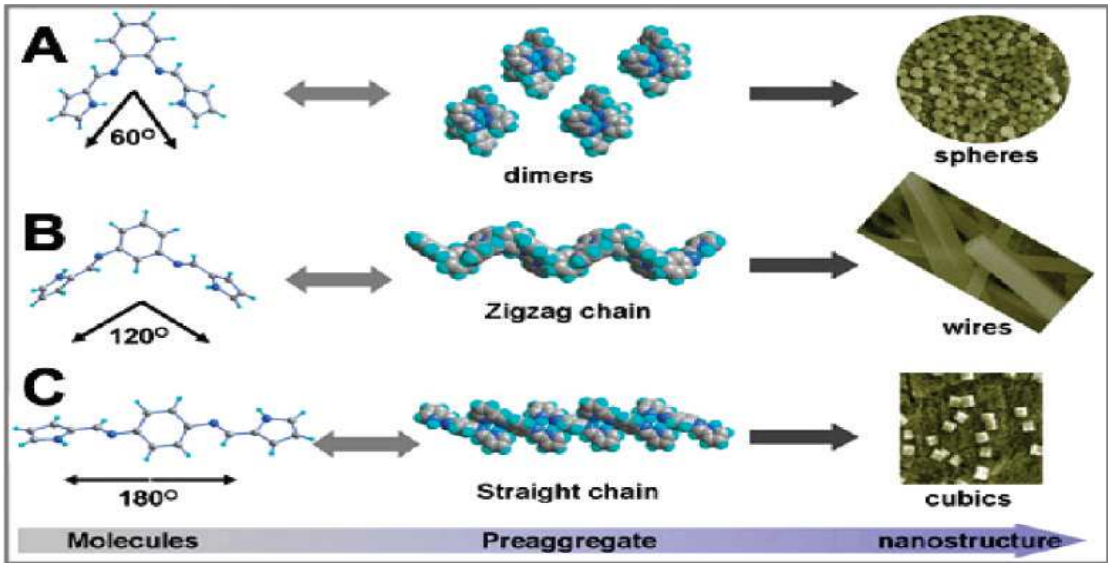

Figure 2.1: Schematic illustration for the formation processes of nanostructures from (A) *o*-, (B) *m*-, and (C) *p*-bis(iminopyrrole) benzene, respectively.[39]

Among these organic nanomaterials, one-dimensional (1D) nanostructures have been specially emphasized, because of their applications as interconnects and functional units in the optoelectronics[40]. Crystalline 1D organic nanostructures offer better stabilities and charge

transport properties and hence better optoelectronic performance[41]. These 1D nanostructures have unique applications, like color tunable display[42], field-effect transistors[43], chemical sensors[44], and lasers[45].

Carbon nanotubes where synthesized by Japanese scientist sumio Iijima in 1991 using arc- evaporation method[46]. Carbon nanotubes can be mainly classified into single wall and multiwall. Carbon nanotubes can be synthesized by arc-discharge[46], laser ablation[47], solvothermal reduction[48] and chemical vapor deposition[49] methods. Carbon nanotubes have applications in field emission, hydrogen storage and solar cells[50]. Carbon nanotubes have physical and chemical properties depend strongly on their diameter and helicity.[51] For example, SWNTs can be metallic or semiconducting, depending on their helicity, which is closely correlated with their diameters.[51]

2.1.1.2 Inorganic nanomaterials

Nanoparticles include metal nanoparticles, metal-oxide nanoparticles or ceramic nanoparticles.

2.1.1.2.1 Metal oxide nanomaterials:

Metal oxides have unique applications including catalysis[52], gas sensors, fuel cell membranes, electro chromic (EC) windows and lithium-ion batteries[53], optics, and electronics[54]. Metal oxide or ceramic nanoparticles have been synthesized using sol-gel[55], metal oxide chemical vapour deposition[56], coprecipitation[57], microemulsion[58], by hydrolysis in polyol medium[59], plasma and decomposition of the precipitates prepared from non-aqueous precipitation routes.

2.1.1.2.2 Metal Nanoparticles:

The brilliant red color of medieval stained glass was due to colloidal gold.[60,61] However, is was not until the mid 19th century that the synthesis of colloidal gold was first reported. M. Faraday reduced gold chloride was reduced by phosphate to produce colloid gold solution.[13] In 1951, Turkevich reported a citrate reduction method in which chloroauric acid is reduced by sodium citrate.[62] Since then metal nanoparticles of Au, Ag, Pd, Cu and Pt have been synthesized using many different synthesis processes.[63, 64, 65, 66] Silver nanoparticles where synthesized by Lee- Miesel method where gold salt is replaced by silver salt in the Turkevich method.[63] Most common method for the synthesis of silver nanoparticles is the reduction of AgNO3 by NaBH4, known as Creighton method.[64] Like the Turkevich method the Creighton method has been extended to other metals such as Pt, Pd, Cu and Ni.[67, 68, 69, 70] More recently methods have been developed to produce nonspherical particles by templating the crystallization processes so that growth is limited in one direction only. These later methods include biological templating[71], wet chemical synthesis[72], template[73], polyol process[74], solution phase[75], and sonochemical synthesis[76].

Metal nanoparticles have unique and distinctive optical, electrical, photo thermal and catalytic properties. Most of these properties depend on size, shape, composition and crystalinity of the particles. For example, the reactivity and selectivity of a nanocatalyst can be tailored by controlling the shape, as it will determine the crystallographic facets exposed on the surface of a nanocrystal and therefore the number of atoms located at the edges or corners[77, 78, 79] There have been many different shapes of metal nanoparticles which have been synthesized as shown in Figure 1.2.[80]

Figure 2.2, shows the different shape particles with single crystals, twin defects or stacking faults, and gold shells. Dark facets are (100) planes, light gray are (111) planes, and {111} twin planes are shown in red. Gold shapes represent gold particles, and gray shapes represent silver particles, although spheres, twinned rods, icosahedrons, and cubes can also be made from gold.

2.1.2 Silver Nanoparticles:

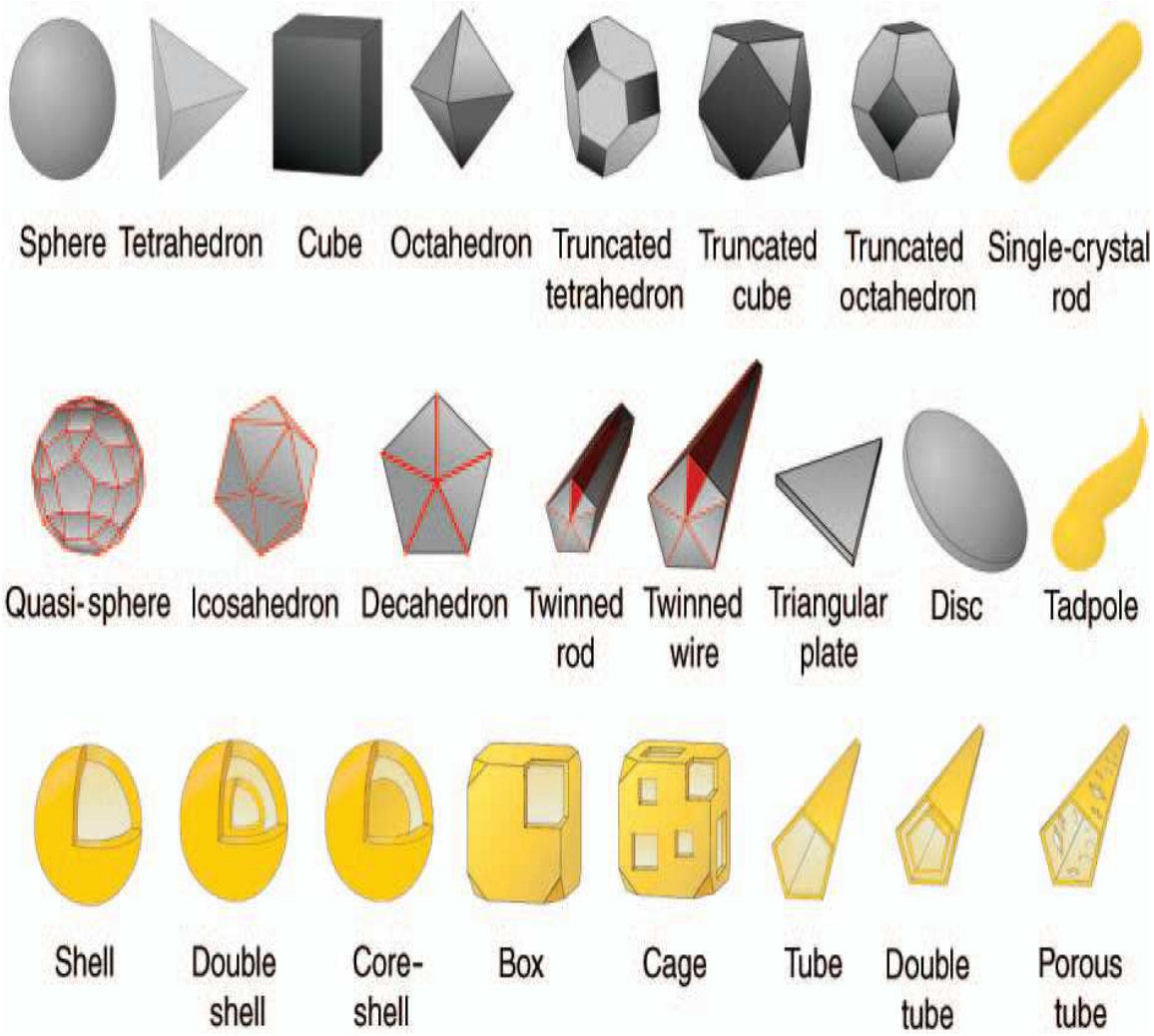

Figure 2.2: **Schematic illustration of nanostructure shapes.**[80]

The focus of this work is on the synthesis and application of silver nanorods and nanowires. Silver is known for its good electrical and thermal conductivity properties and its optical and antimicrobial properties are enhanced at small size scales. Silver nanoparticles exhibit a high efficiency of plasmon excitation compared to Au and Cu.[2] and therefore have potential application as chemical and biological sensors. Silver nanoparticles have traditionally been synthesized by Creighton method. Modifications to this basic method include changing the silver salt or reducing agent.[81, 82, 83, 84, 85, 86, 87, 88]

All bottoms up chemical synthesis of silver nanoparticles starts with the reduction of a silver salt. The reduced Ag forms nuclei crystals which tend to agglomerate. To avoid agglomeration surfactants or capping agents are used. By utilizing capping agents that preferentially bind to one crystal face and block growth of this face directed growth can be effected.

Silver nanoparticles can also be synthesized using template technique[89], porous materials templating, biochemical[90], γ- radiation[91], laser ablation[92], solvothermal[93], electrochemical[94], polyol[95], electric discharge method[96], wet chemical[97], sonochemical[98] and photochemical methods[99]. Among these methods, Polyol is the most widely used method. Polyol method was developed by Fievet and co-workers[100] and has been used for the synthesis of nanoparticles of many metals and alloys of Ag[95], Au[101], Cu[102], Co[103], Ir, Ni[104], Pd[105], Pt[106], Ru[107], CoNi and FeNi[74].

2.1.3 Polyol Process:

In a typical polyol process, inorganic salt is reduced by the polyol at a high temperature (near boiling temperature). In most of the synthesis methods, the polyol used is generally ethylene glycol; this ethylene glycol serves as both solvent and reducing agent.

In polyol process, the salt precursor is reduced from silver ions (Ag^{+}) to silver (Ag^{0}) by the acetaldehyde. Acetaldehyde is produced from ethylene glycol on heating. When the silver atom reaches super saturation, they agglomerate to form nuclei and seed crystals are formed. For narrow distribution, homogeneous nuclei (or seed) formation is required. The seed formed play a major role in the formation of anisotropic structures. Figure 2.3 shows the formation of different seed structures, which lead to different structures of silver nanoparticles.[108]

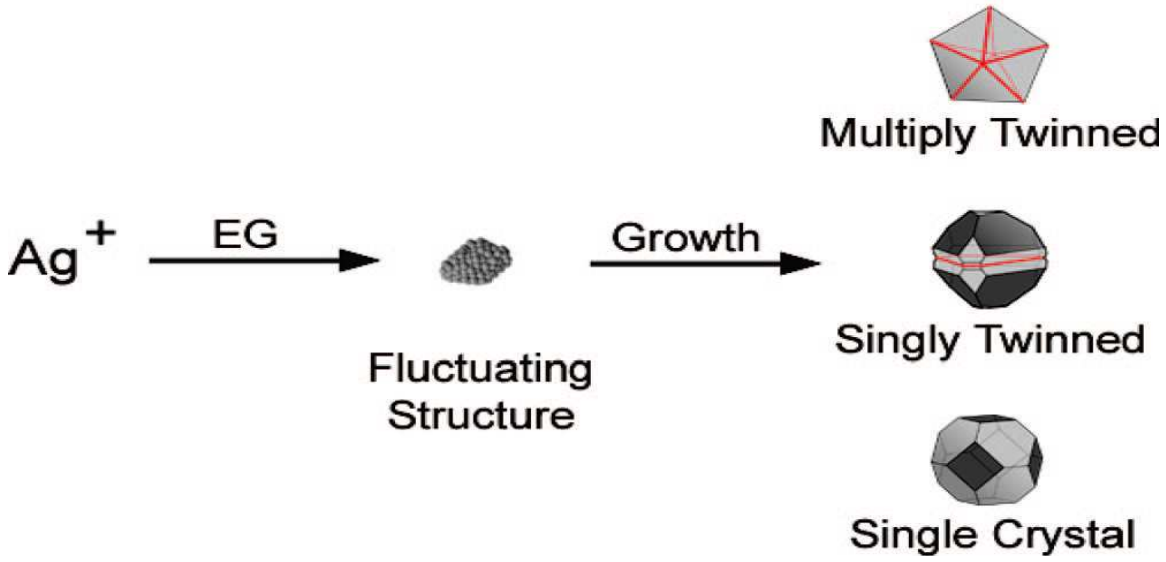

Figure 2.3: Reduction of Ag+ ions by EG leads to the formation of nuclei.[108]

The structure of nuclei fluctuates depending upon their size and the thermal energy available. Most nuclei contain twin boundary defects because such defects enable a lower surface energy. As nuclei grow, fluctuations cease and they are stuck as a multiply twinned, singly twinned, or single-crystal seed. Different seeds then grow into nanostructures with different

shapes; therefore, one must regulate the crystalinity of the seeds in a reaction to produce a specific shape. The crystalinity of the seeds can be controlled by the salts used. These salts electrostatically stabilize the structure of the nuclei, which help to grow into a particular shape seed. Some of the salts used for the synthesis of silver nanoparticles are NaCl, Na_2S, $FeCl_3$, and $CuCl_2$.

The formation of different seed structures is due to the crystalinity of the seeds. The different seed shapes like multi twinned (decahedral seeds), single twinned and single crystal seeds grow into nanowires or nanorods, right bipyramids or nanobeams and nanospheres respectively.

Surfactants are used for steric stabilization of nanoparticles. Poly (vinylpyrrolidone) (PVP) is the most used surfactant in the synthesis of silver nanoparticles through polyol method. PVP has been widely used as a protecting agent for silver nanoparticles in the liquid state to avoid their aggregation,[109, 110, 111] because it shows better stabilizing properties than the other widely used substances used as stabilizer such as alcohols, thiols, dendrimers, and surfactants.[112] PVP is a homopolymer with a polyvinyl backbone and its repeat unit contains an amide group as shown in figure 2.4. These structural features make this polymer a good stabilizing agent for transition metal particles and especially for noble metal nanoparticles.[113, 114, 115]

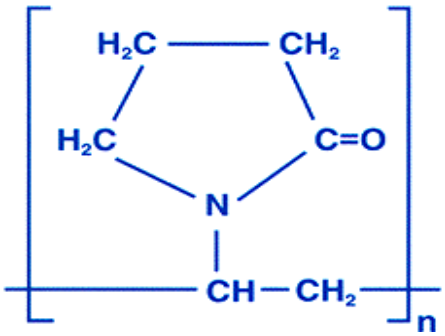

Figure 2.4: Structure of Poly (vinylpyrrolidone)[116]

2.1.4 1-Dimensional silver nanoparticles:

Among all the different shapes of silver nanoparticles, 1-Dimensional nanostructures have attracted a lot of attention due to their distinctive properties and applications. 1D silver nanoparticles have unique optical[117], electrical[118], and thermal[119] properties. Indeed, these properties give 1D silver nanostructure applications in surface enhanced Raman scattering (SERS)[120], catalysis[121], photonic crystals[122], and biological nanosensors[123].

1D silver nanoparticle includes nanorods, nanowires and nanotubes. These 1D structures are synthesized in many different methods like template method[124], wet chemical method[125], solvothermal method[126], and polyol method[127]. Most of the silver nanorods and nanowires have been synthesized using polyol process.

Figure 2.5 shows the mechanism of formation of silver nanowires from twinned decahedral seeds. Once twinned decahedral seeds lengthened into rods. PVP selectively adsorbed on the {100} side facets so that Ag atoms could only add to the {111} facets at the ends of each rod. PVP has a more tendency to interact with the {100} side facets than the {111} facets due to its structure. All the sides are covered by the PVP, only {111} facet side is available for the silver atoms to combine. This mechanism tends to result in the formation of silver nanorods or nanowires.

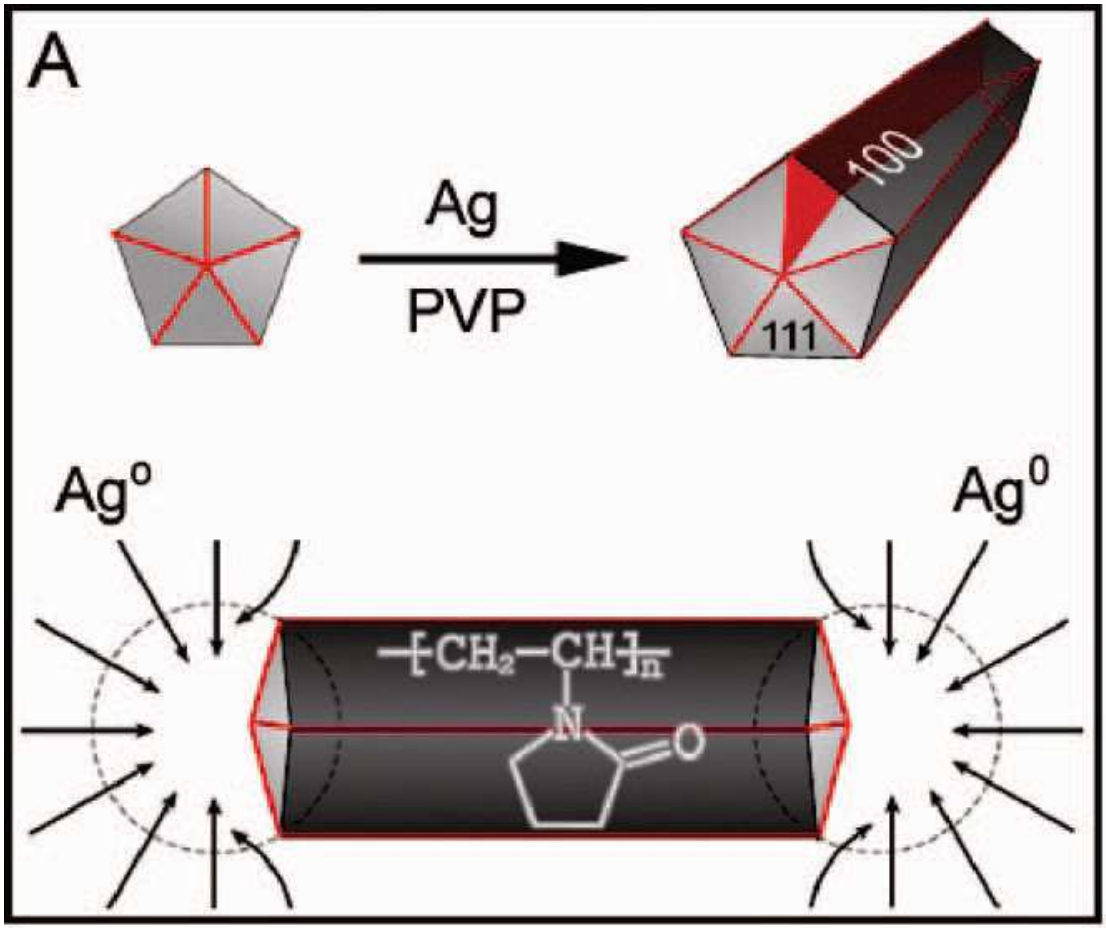

Figure 2.5: **Schematic illustration of mechanism proposed to account for the growth of silver nanowires.**[108]

Conventional polyol process takes long reaction times but with improvements in the method of heating, the reaction time has now come down to minutes. Xia et. al has produced silver wires in just 1 hour. Recently, Gou et al has prepared silver nanowires within 3.5 minutes using microwave[128]. There are many advantages of using microwave over conventional methods in synthesis are (a) the kinetics of the reaction are increased by 1-2 orders of magnitude,[129] (b) novel phases are formed[129] (c) the initial heating is rapid which can lead to energy savings, and (d) selective formation of one phase over another occurs.[130] One possible hypothesis for the microwave induced effects is the generation of localized high temperatures at the reaction sites to

enhance reaction rates in an analogous manner to that of ultrasonic waves where both high temperatures and pressures have been reported during reactions. The enhanced kinetics of crystallization which can lead to energy savings of up to 90% and the environmentally benign closed system condition of the Microwave Polyol process is ideal for the synthesis.

Only NaCl and Na2S salts have been studied using microwave polyol process. As mentioned earlier, in this work the effects of other salts on the synthesis of the silver nanorods have been explored. In addition effects of container shape, effects of mixing methods, effects of concentration of salt and continuous synthesis of silver nanoparticles have also been studied.

2.1.5 Effect of shape of container:

Silver nanowires have been synthesized in different shape containers like flask, glass vial and 3 necked flasks. In most of the synthesis processes, shape of the reaction container is not mentioned. Gou et. al, has used a flask for the synthesis of silver nanowires through microwave assisted polyol method[128]. Chen et al and Korte et al have used three necked flask and glass vial respectively for the synthesis of silver nanowires through conventional polyol method[131,132]. In all the previous work, no one has mentioned the dimensions of the reactor or container shape. In case of microwave assisted synthesis, the shape of the container and mass of the container are important. The container does absorb the energy and the area of the solution directly exposed to air can affect the yield of the silver nanowires. To the best of our knowledge there has not been any previous work on the effect of shape of container on the synthesis and yield of the silver nanoparticles.

2.1.6 Continuous flow synthesis:

Synthesis of nanoparticles in a continuous process had been in research interest recently. There is a very little work done on this topic in case of metal nanoparticles. Initially, much

interest was on semiconducting materials like CdSe[133] and TiO2[134] in continuous flow process, in a fluidic micro-reactor. Wager has produced gold nanoparticles in a continuous flow tubular system.[135] As shown in Figure 2.6, Lin et al has synthesized silver nanoparticles in a continuous process using tubular coil made of stainless steel needle in an oil bath.[136]

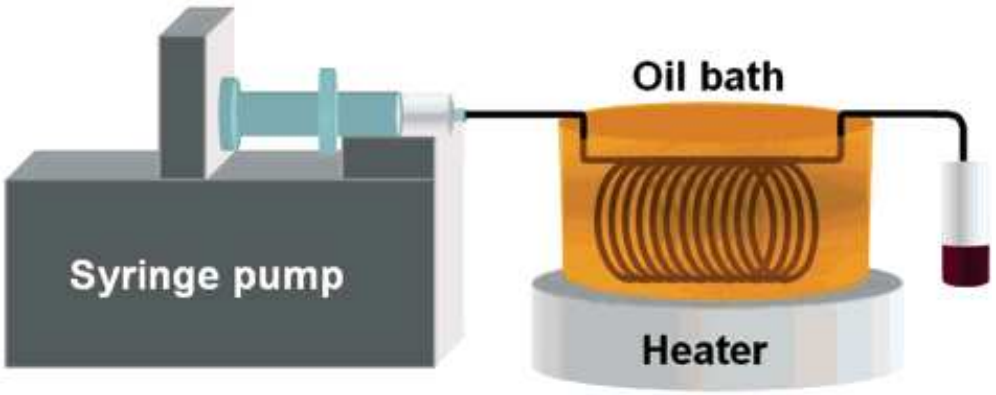

Figure 2.6: Experimental setup of the synthesis of Ag nanoparticles in a tubular microreactor.[136]

In 2005, Kohler et al has synthesized gold nanoparticles in a Silicon and Pyrex glass chip micro-reactor under continuous flow process.[137] Tai et al has synthesized silver nanoparticles in a continuous process using spinning disk reactor.[138] The yield was less in continuous mode when compared to their previous work in recycling mode but production rate increased 5 to 6 times using the same spinning disk reactor. Till now no one has synthesized silver nanowires from continuous synthesis process. In this work, silver nanowires in continuous flow process were tried to synthesize using microwave.

2.1.7 Effect of alkali and alkaline earth metal salts:

Polyol process has been used for the synthesis of silver nanoparticles. The standard polyol process requires careful control over reaction rates to tailor the particle geometry. Several "control" agents have been examined in the traditional polyol process for their ability to control

particle geometry. Chen et. al. has reported the synthesis of silver nanowires with different diameters using different control agents like KCl, KBr, KOH, $Fe(NO_3)_3$, $PdCl_2$, Na_2S and ascorbic acid.[131] The alkali and alkali metal salts used as control agents are NaCl, KCl and Na_2S. Chen et. al. has reported the effect of Na_2S salt, where silver nanocubes and nanowires where produced at 62.5-250µM and 750µM concentration of Na_2S salt respectively. This clearly shows that the concentration of salt does affect the morphology of the product.

To speed the reaction time of the polyol process microwave heating has been used to rapidly heat the reactants and reduce overall reaction time to less than 5 min.[128] Two anions have been evaluated in the microwave assisted polyol process, Cl^- and S^-.[128,139] They form AgCl salts or Ag_2S colloids and limit the amount of Ag^+ ions present in the solution that can be reduced to Ag^0, effectively controlling the overall formation of Ag^0 thus allowing for directed growth to occur without the continued formation of new nuclei. In the case of Na_2S a wide variety of shapes including rods and cubes have been synthesized. As noted, several studies have found that significant control over the rod morphology can be obtained in the "traditional" process by utilizing different cations. However, the effect of these cations on product geometry in the microwave assisted polyol synthesis process has not been reported. To date the only cation that has been evaluated in the microwave assisted process is Na. Several different cations were evaluated in this work in an effort to see if the control over the particle geometry noted in the traditional polyol synthesis can be achieved in the microwave assisted process. A range of alkali salts were evaluated including NaCl, KCl, $MgCl_2$, $CaCl_2$.

2.1.8 Effect of transition metal salts:

In contrast the polyol process results in rods suitable for several applications, but the standard process requires careful control over reaction rates to tailor particle geometry. Several

morphologies can be produced by controlling reaction conditions such as the concentration of Cl^- and H^+, temperature, presence or absence of O_2, and by controlling the reaction rate by drop wise addition of reactants. [140,141] Several "control" agents have been examined in the traditional polyol process for their ability to control particle geometry. Fe (II) was reported by Wiley et. al. to control the reaction through the oxidative etching of the silver seeds.[141] Figure 2.7 shows the mechanism of removal of atomic oxygen from the surface of silver atoms by Fe (II). Reduction by ethylene glycol (EG) competes with oxidation by atomic oxygen to form an equilibrium between Fe(III) and Fe(II). Chen et. al. later demonstrated the reduction in silver nanowires diameter by the addition of $Fe(NO_3)_3$.[131] This effect has been explained through the process of etching the silver surface, the removal of oxygen from the surface, or the ability of metals with multiple valence states to affect the reduction of Ag^+. Other control agents that have been examined include salts of potassium, copper, and palladium, and sodium sulfate.[131, 141,142,132]

To our knowledge, in case of transition metals there has not been any work reported for the synthesis of silver nanostructures through microwave assisted polyol process. Several different transition metal cations were evaluated in this work in an effort to see if the control over the particle geometry noted in the traditional polyol synthesis can be achieved in the microwave assisted process. A range of transition metal salts were evaluated including FeCl3, CuCl2, MnCl2. The effect of concentration of salt on the final morphology of the silver nanoparticles was also evaluated.

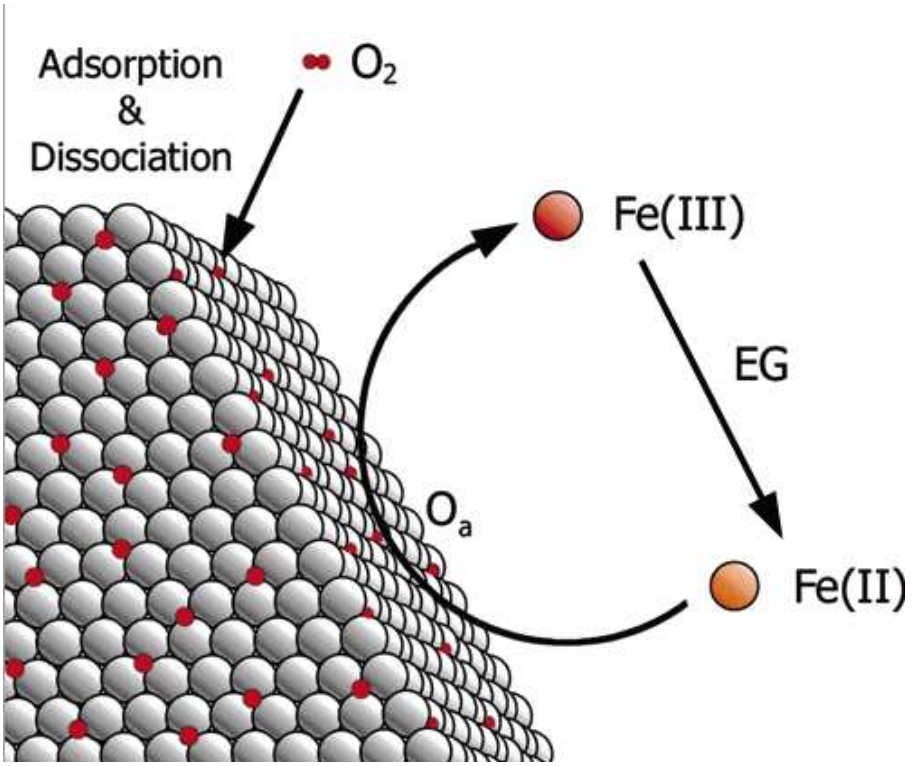

Figure 2.7: Illustration of the proposed mechanism by which Fe(II) removes atomic oxygen from the surface of silver nanostructures.[141]

2.1.8 Effect of mixing methods:

Change in the order of addition and mixing method can influence the final morphology and yield of nanoparticles. Gou et al has used sonication method in order to speed the dissolution of solid powders[128]. Chen et al has produced different morphologies using different control agents but under argon gas in order to have repeatability and also to avoid oxidative etching[131]. To the best of our knowledge there has not been any work done in this aspect of mixing methods and shielding atmosphere. At the initial work, mixing of the final stock solutions was not given importance and the results we got were not repetitive. This has lead to the study of the effect of mixing on the final morphology and yield of the silver nanoparticles.

Chapter 3

Materials and Methods

3.1 Materials Used:

Silver nitrate (AgNO3, >99%) was purchased from Sigma Aldrich, Poly (vinyl Pyrrolidone) (PVP, MW≈ 58k) from Acros Organics, Ethylene Glycol (EG, >99%) and salts NaCl, KCl, MgCl2, CaCl2, MnCl2, CuCl2 and FeCl3 were purchased from Fisher Scientific and all the chemicals where used as received. Two microwaves were used in this work, one is from Microwave Research Labs (model BP 211) of 3200W continuous power and the other microwave used is a commercially available microwave (General Electric model JES1855) of power 1100 W.

In case of effect of shape of the reaction vessel, all the chemicals are same but only NaCl salt was used. Three different reaction vessels where used with different shapes. Those are a (5 cm diameter X 19.5 cm) glass beaker, a (7cm diameter X 10cm) glass beaker and a (10 cm diameter X 5 cm) glass crystallization dish.

For continuous flow synthesis process, all the chemicals used are same. The microwave used was from Microwave Research Labs (model BP 211) of 3200W continuous power. In this process a glass tube of 2cm diameter as shown in figure 3. The pump used is High performance digital peristaltic pump from Peri-Star Pro (model LEAD 15-48).

In case of effect of alkali and alkaline earth metals, all the chemicals used are same except the salts. The salts used are NaCl, KCl, MaCl2, CaCl2 were purchased from Fisher

scientific and used as received. The microwave used is a commercially available microwave (General Electric model JES1855) of power 1100 W.

In case of effect of transition metal salts on synthesis of silver nanorods, all the chemicals used are same except the salts. The salts used are MnCl2, CuCl2 and FeCl3 were purchased from Fisher scientific and used as received. The microwave used is a commercially available microwave (General Electric model JES1855) of power 1100 W.

For effect of mixing methods, all the chemicals used were same except the salt. The salt used was KCl and was purchased from Fisher scientific. All the chemicals were used as received. The microwave used is a commercially available microwave (General Electric model JES1855) of power 1100 W.

3.2 Synthesis:

Three stock solutions were prepared separately; one with AgNO3 in 20ml EG of 0.026M concentration, PVP in 20ml EG of 0.05M concentration, NaCl in 20ml EG of 4.3mM concentration. All stock solutions were prepared just prior to use and sonicated to aid dissolution until uniform dispersion of the solutes are obtained. After preparation of the three solutions 20 ml of the PVP solution was placed in the reaction vessel followed immediately by 20 ml of the $AgNO_3$ solution, and then by 20 ml of the salt solution, total reaction volume was 60 ml. Immediately upon the addition of the salt solution, the entire solution becomes opaque with an opalescent color due to the formation of AgCl colloidal particles. The solution was mixed by swirling the container for 10 – 15 seconds. The solution was then transferred to the microwave oven operating at 620W (10% power level of microwave) and heated for 42 seconds. Upon completion of the reaction, solutions were allowed to cool in air for 40 minutes. Samples were taken immediately after cooling for characterization.

Figure 3.1 shows the set up of the continuous synthesis process for silver nanoparticles. The stock solutions where prepared for a total of 180 ml. Each AgNO3, PVP and salt NaCl 60 ml with concentrations of 0.026M, 0.05M, 4.3mM respectively. The pump was operated at three different speeds 8, 10 and 12ml/minute for a resulting residence time of 75, 60 and 50 seconds respectively. The solution was pumped through the glass tube in the microwave operated at a power of 1060W (20% on power dial).

In this continuous synthesis process, stable temperature was obtained at different timings according to the flow rate unlike other continuous process. For 12ml/min flow rate a stable temperature of 139^{o}C was obtained after 10 mins. For 10ml/min flow rate a stable temperature of 134^{o}C was obtained after 8mins. And for 8ml/min flow rate stable temperature of 125^{o}C was obtained after 5 minutes. Upon achieving a stable temperature, the product was collected at the other end of microwave and allowed it to cool in air for 40minutes.

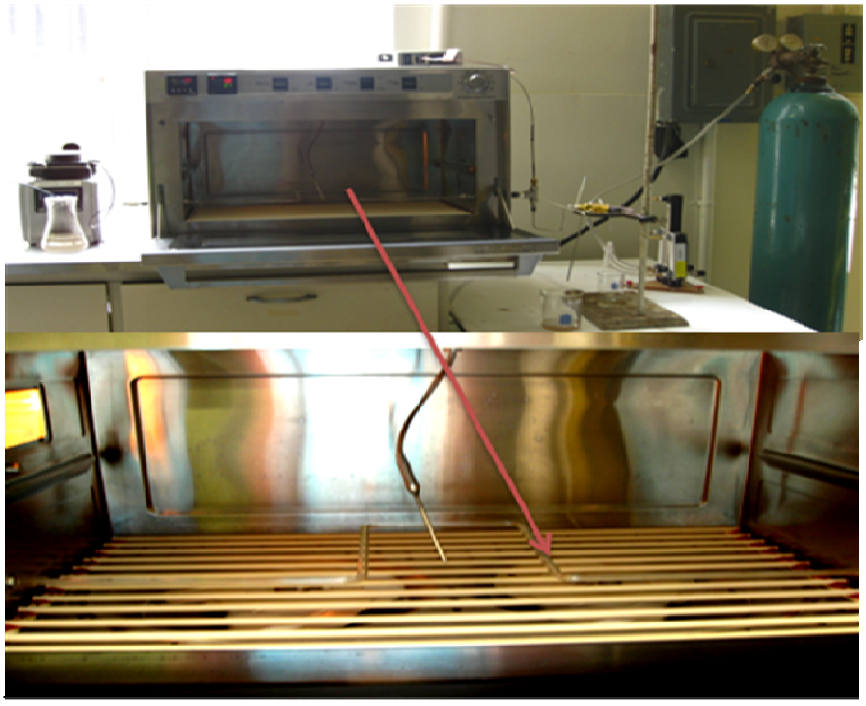

Figure 3.1: A) Reaction set up of the continuous synthesis of silver nanoparticles, B) Closer look at the glass tube in the microwave

Figure 3.2 shows the schematic of the synthesis process, characterization and evaluation of the product for effect of alkali and alkaline earth metals and transition metals. Synthesis procedure was similar to the effect of container shape except the microwave used and the salts. After mixing the 3 stock solutions, the final solution was then purged with nitrogen gas for 1 minute at 20 psi flow rate. This solution was then transferred to the microwave oven operating at 350W (4th power level of microwave) and heated for 2 minutes. Upon completion of the reaction, solutions were allowed to cool in air for 40 minutes. Samples were taken immediately after cooling for characterization.

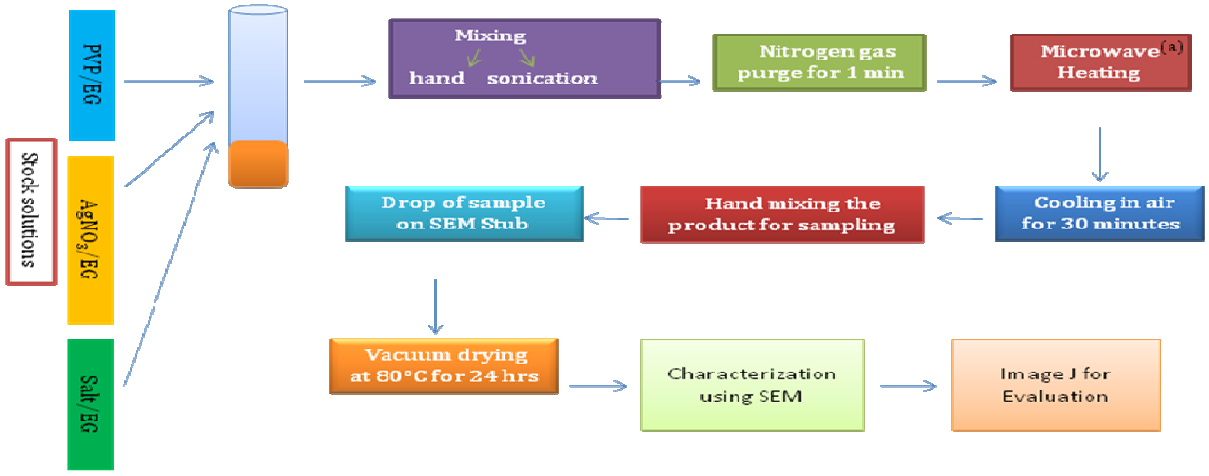

Figure 3.2: Schematic representation of synthesis, characterization and evaluation. (a) Microwave heating for 2 minutes at 350 Watts power, where the microwave is on for 13 seconds and off for the next 17 seconds.

In case of effect of mixing methods, the synthesis method is similar to the synthesis method mentioned in the effect of container shape except the mixing methods. Table 3.6 shows the different mixing methods and after the mixing, the solution was then transferred to the microwave oven operating at 350W (4th power level of microwave) and heated for 2 minutes. Upon completion of the reaction, solutions were allowed to cool in air for 40 minutes. Samples were taken immediately after cooling for characterization.

3.3 Characterization:

All the reaction products were air cooled for 40 minutes prior to sampling. The reaction product was mixed by swirling the container for 30 sec just prior to sampling with disposable transfer pipette.

The products obtained from the synthesis of different shape containers where characterized using TEM and optical microscope. Drops of the reaction product were placed on 100 mesh copper grid with carbon tape and vacuum dried at 80 ºC for 24 hours to remove EG. The samples were characterized using a Ziess Transmission Electron Microscope (TEM) at 60 kV. Images at 12.5K magnification where taken.

Optical microscope was used to take the images of silver nanowires and atleast three images where taken for counting. Image-Pro PLUS analysis of optical microscope images taken on a Nikon Eclipse 80i at 60x magnification with 1.4 NA was performed to count rods and spheres in the reaction product.

The products obtained from continuous flow synthesis where characterized using FESEM. Drops of the reaction product were placed on aluminum stubs with carbon tape and vacuum dried at 80 ºC for 24 hours to remove EG. The samples were characterized using a JEOL 7000 Field Emission scanning electron microscope (FESEM) at 20 kV. The samples were not gold sputtered. While silver is conductive PVP is not. This results in hazing of the PVP layer in the images. High magnification images (70k magnification) were used to determine the diameters. The number of particles present in a 2 by 3 micron grid was determined in a 35k magnification image and used as a measure of particle yield. Multiple images were taken at each magnification, at least three, for each sample to account for sample variability across the stub.

The products from the alkali and alkaline earth metal salts where characterized using FESEM images at 3 different magnifications. Drops of the reaction product were placed on aluminum stubs with carbon tape and vacuum dried at 80 ºC for 24 hours to remove EG. The samples were characterized using a JEOL 7000 Field Emission scanning electron microscope (FESEM) at 20 kV. The samples were not gold sputtered. While silver is conductive PVP is not. This results in hazing of the PVP layer in the images. High magnification images (35k magnification) were used to determine rod diameters. To measure length lower magnification images (5k magnification) were used. The number of rods or wire present in a 2 by 3 micron grid was determined in a 20k magnification image and used as a measure of rod yield. All rods that intersected the measurement area were counted. Multiple images were taken at each magnification, at least three, for each sample to account for sample variability across the stub.

Chapter 4

Results and Discussion

4.1 Effect of shape of the container on synthesis of silver nanorods:

Three containers were evaluated to determine if the surface area of the reaction played a role in the rate of formation of the reaction, as shown in Figure 4.1. The determined rod to sphere number ratio is provided in the inset table of Figure 4.1. The vessel with the largest diameter, thus the largest surface area, produced no rods when imaged. As the container diameter was decreased the number of rods increased. The source of this variation is not clear at this time; however a few possible reasons were explored. Figure 4.2 shows the TEM images of the samples.

One possible reason for the change in performance is that the irradiation level was not consistent within the microwave cavity. To test this hypothesis the reaction was repeated multiple times using the large crystallization dish at various locations within the cavity. Rods were not produced at any location.

Changing the geometry of the vessel changes the open surface area, the mass of glass used (all containers were fabricated with the same wall thickness), and the surface to volume ratio of the reaction volume. The open surface area affects the vaporization rate. The mass of glass used may affect the fraction of energy lost to heating the container. The surface to volume ratio of the reaction mass will affect the heat distribution within the volume at short times, before convective heat transfer starts, and the cooling rate of the reaction mass after removal from the microwave.

To test the effect of limiting the vaporization rate, test were performed with a watch glass placed on the open surface of the container to limit vaporization. This did not affect the rate of rod formation.

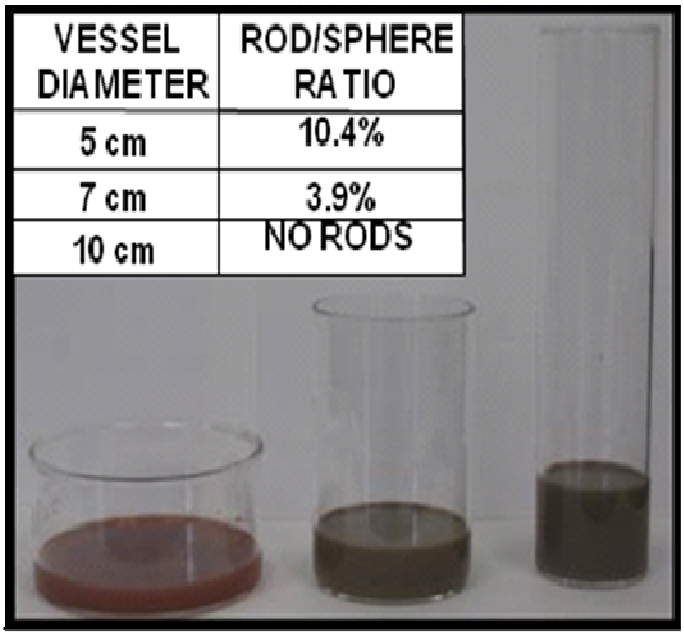

Figure 4.1: Comparison between three container shapes evaluated in initial work. The containers total volume was the same, 300 ml, in all cases.

The change in total mass of glass is an increase of ~30% going from the highest diameter to the lowest diameter vessel used in this study. To see if this was affecting heat up rates during the reaction temperature monitoring was performed for all three reactors. Difference in the reaction temperature was observed. A temperature of 127^{o}C, 123^{o}C and 117^{o}C was obtained in case of 5cm, 7cm and 10cm diameter glass beakers. The mentioned temperatures were measured immediately after taken out from the microwave. This difference in the final temperatures can be one of the reasons for different rods/ spheres ratio.

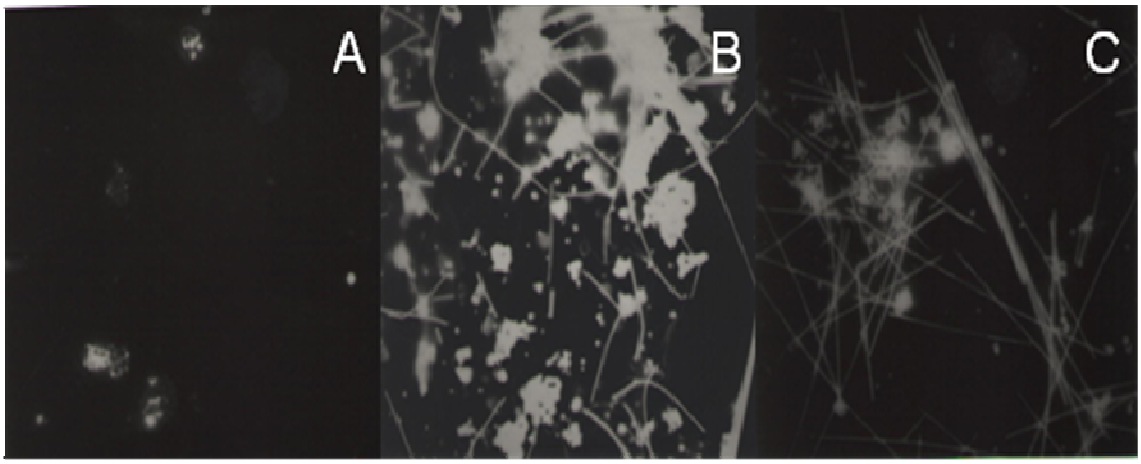

Figure 4.2: TEM images (12.5K) of Silver nanostructures formed at 600W in 42s A) 5cm diameter, B) 7cm diameter, and C) 10cm diameter glass beakers.

Figure 4.2 shows the TEM images of the silver nanoparticles synthesized from different shape containers. The container with 10cm diameter has resulted in no rods (Figure 4.2A) and the container with 7cm diameter has produced the nanorods but less in yield compared to 10cm diameter container. The final effect relates to how the initial reaction is distributed throughout the reaction volume. As the irradiation is attenuated by absorbance by the reactants, the power level drops from the outside of the reaction volume towards the center of the reaction volume. One might expect that a more even heating would result in better performance. However, the container that should have the most even heating of the reactants, the large diameter vessel, resulted in the lowest production of rods. As the small diameter vessel produced the highest number of rods in these early tests it was used exclusively for the remainder of the experiments herein discussed. The source of the variability in rod yield as a function of container geometry will require further investigation.

4.2 Continuous flow synthesis of silver nanoparticles:

Figure 4.3 shows the SEM images of the silver nanoparticles produced through continuous flow process using a microwave. Three different flow rates, 8ml/min, 10ml/min and 12ml/min have been used with a residence time of 75, 60 and 50 seconds. The white big structure seen in all the SEM images is PVP.

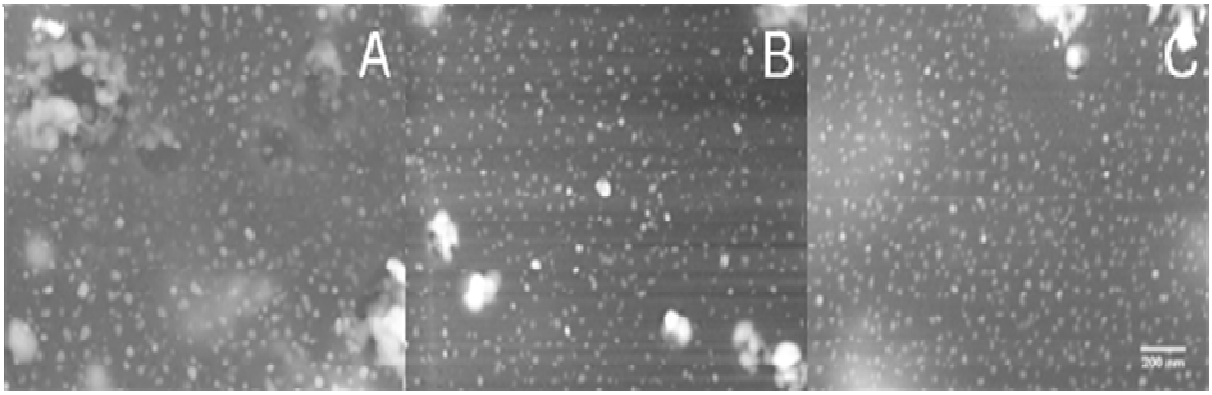

Figure 4.3: SEM images of silver nanoparticles in a continuous flow microwave synthesis at 3 different flow rates A) 8ml/min, B) 10ml/min, C) 12ml/min.

Table 4.1 shows the diameter and number of nanospherical particles produced. As the flow rate increases, the particle size decreased due to greater nucleation rates than the growth rate where the growth rate would have repressed.[136] Low flow rates give larger particle size as there is enough residence time for the growth of the particles.

Table 4.1: Particle diameter and # produced for continuous flow synthesis.

		Concentration (nM)			Ag Rod / Wire Properties Mean and (Std. Dev.)	
Salt	**Cl^-: $AgNO_3$**	**Metal**	**Chlorine**	**Flow rates (ml/min)**	**Diameter (nm)**	**# of spheres[a]**
NaCl	1:6	4.3	8.6	8	27.2 (7.1)	147 (9)
				10	21.3 (4)	180 (15)
				12	20.57 (8.2)	216 (12)

A) Count of spheres in 2 by 3 micron area from SEM images.

At low flow rate the reduction of Ag- to Ag0 preferentially takes place at the walls of the tube as the surface of tube itself acts as nucleation site. This process can be clearly indicated by the formation of thin silver film on the inner wall of tube of orange color. As the synthesis proceeds further, the film becomes grey in color and then to opaque indicating the silver particles aggregation on the film. If the glass tube and bearings are not cleaned properly, after few experiments, the flow will be blocked by the accumulated silver nanowires. At high flow rates the thin film formation is not seen at that fast rate compared to low flow rate synthesis. This might be due to the less surface interaction because of high surface sheer energy at higher flow rates.

4.3 Effect of alkali and alkaline earth metal salts on the synthesis of silver nanorods:

The effect of the cations Na, Ca, Mg, and K was evaluated by preparing parallel solutions of the chloride salts of the metals in EG and using this as the chloride source for the reaction. Gou reported that the most favorable Cl^- to $AgNO_3$ ratio for the synthesis was between 1:6 and 1:3.[128] For the Na and K a ratio of 1:6 was evaluated while for Mg and Ca both 1:6 and 1:3 ratios were evaluated. Figure 4.4 shows representative samples of the highest magnification SEM images taken; these images were used to evaluate the rod diameter.

Table 4.2 provides the diameters, lengths, and rod counts for all salts evaluated in this study. Of the four salts evaluated from group one and group two Mg had the most significant effect on the rod diameter. The rod diameter decreased from ~ 38 to 31 nm when changing the salt from NaCl to $MgCl_2$. In contrast changing the salt to KCl reduced the mean diameter to only 35.6 nm and the use of $CaCl_2$ increased the rod diameter and the overall distribution.

Table 4.2: Rod diameter, length, and # produced for alkali salts evaluated.

		Concentration (nM)			Ag Rod / Wire Properties Mean and (Std. Dev.)			
Salt	**Atomic Radius Metal (pm)**	**Metal**	**Chlorine**	**Cl:$AgNO_3$ Ratio**	**Diameter (nm)**	**Length (μm)**	**Nominal AR[a]**	**# of rods[b]**
NaCl	186	4.3	4.3	1:06	38.6 (9.1)	7.6 (1.6)	197	60 (12)
KCl	227	4.3	4.3	1:06	35.6 (9.0)	9.1 (1.7)	255	51 (5)
$MgCl_2$	160	2.15	4.3	1:06	31.4 (4.5)	3.7 (1.5)	118	49 (12)
		4.3	8.6	1:03	26.1 (6.7)	1.2 (0.5)	46	12 (5)
$CaCl_2$	197	2.15	4.3	1:06	41.0 (13.2)	7.4 (1.9)	180	58 (13)
		4.3	8.6	1:03	35.8 (8.8)	8.5 (2.2)	237	30 (4)

A) Based on mean length and diameter.
B) Count of Rods in 2 by 3 micron area from SEM images.

At a Cl^- to Ag ratio of 1:6 the longest rods were obtained from KCl and the highest number of rods was obtained from NaCl. Changing the Cl^- , Ag ratio to 1:3 for $MgCl_2$ and $CaCl_2$ affected the diameter, length, and rod number. Higher $MgCl_2$ concentrations resulted in significantly fewer, much shorter, and smaller diameter rods, aspect ratio (AR) ~ 46. A similar change with $CaCl_2$ however resulted in fewer, slightly longer, smaller diameter rods, AR ~ 247. Clearly the effects of concentration are different between these cations.

To see the effect of concentration of salt on the morphology of the silver nanoparticles, six different concentrations were synthesized. MgCl2 salt was considered with 6 different concentrations, as shown in Table 4.3 for this study.

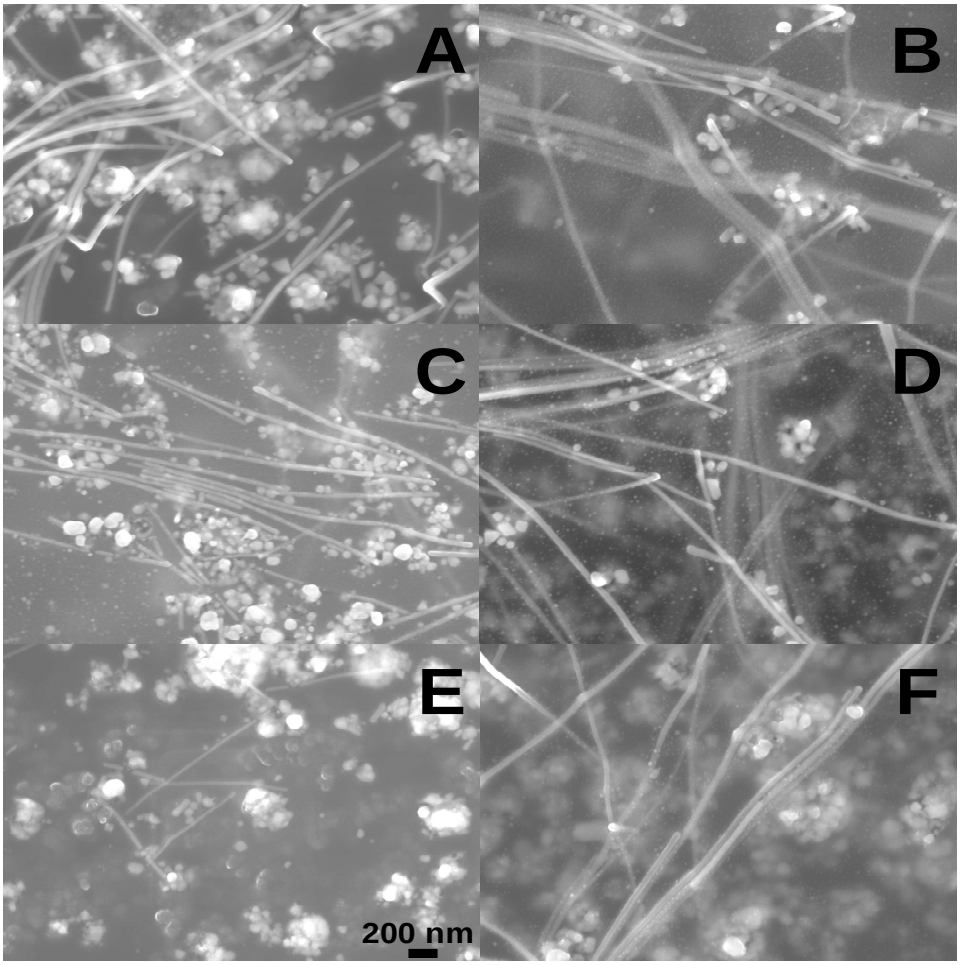

Figure 4.4: SEM images of silver nanoparticles produced using group one and group two metal chlorides: A) NaCl, B) KCl, C and E) $MgCl_2$, D and F) $CaCl_2$: A, B, C, and D) at 4.3 mM concentration: E and F) at 8.6 mM.

Figure 4.5 shows the SEM images of silver nanostructures formed from different concentrations of MgCl2 salt. MgCl2 at 1.075mM concentration has produced maximum number of rods with an aspect ratio of ≈209.The highest aspect ratio of ≈255 was achieved at 3.225mM concentration. The different salt concentrations did not show any specific pattern. At higher concentration much of spherical particles where formed, this might be due to the etching of silver by excess Cl^- ions. Different salts have different optimum concentrations to obtain nanorods.

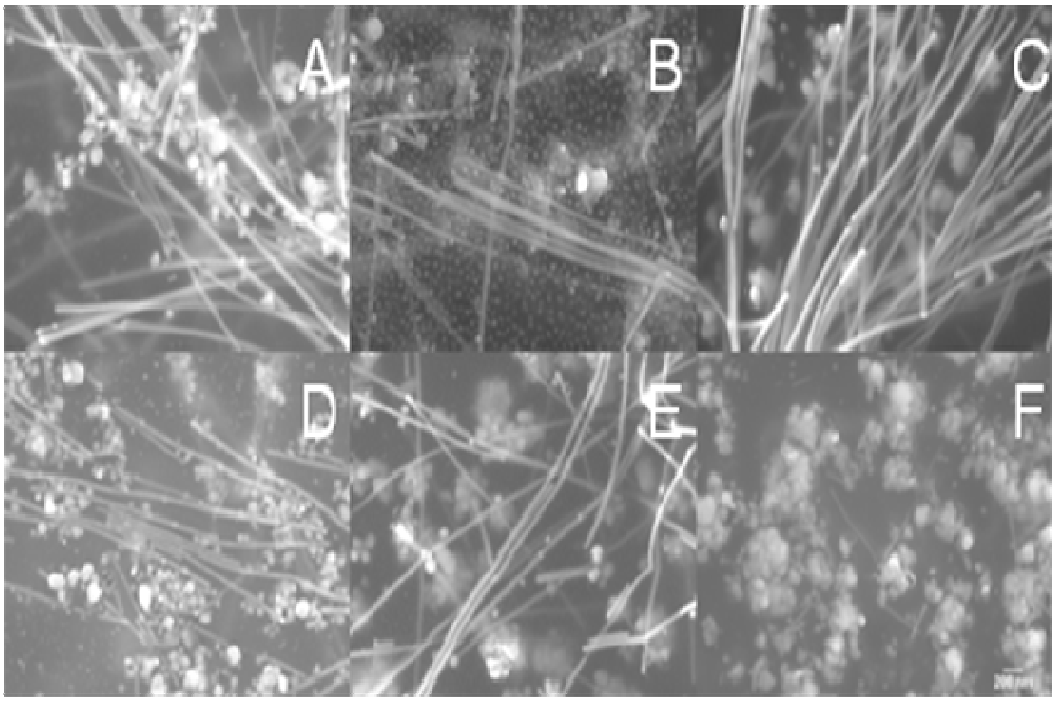

Figure 4.5: SEM images of silver nanoparticles using MgCl2 salt at A) 0.268mM, B) 0.537mM, C) 1.075mM, D) 2.15mM, E) 3.225mM, and F) 4.3mM

Table 4.3: Rod diameter, length, and # produced for effect of concentration of alkaline earth metal salt ($MgCl_2$) evaluated.

		Concentration (mM)			Ag Rod / Wire Properties Mean and (Std. Dev.)			
Salt	**Atomic Radius Metal (pm)**	**Metal**	**Chlorine**	**Cl:$AgNO_3$ Ratio**	**Diameter (nm)**	**Length (μm)**	**Nominal AR[a]**	**# of rods[b]**
$MgCl_2$	160	0.268	0.537	1:48	36.4 (7.1)	7.2 (2.3)	197.8	50 (17)
		0.537	1.075	1:24	39.2 (6.2)	7.3 (2.7)	186.2	28 (6)
		1.075	2.15	1:12	35.4 (9)	7.4 (1.8)	209	80 (13)
		2.15	4.3	1:06	31.3 (4.5)	3.7 (1.5)	118.2	50 (12)
		3.225	6.42	1:04	33 (10.7)	8.4 (2.5)	254.5	45 (13)
		4.3	8.6	1:03	26.1 (6.6)	1.2 (0.5)	45.9	12 (4)

A) Based on mean length and diameter.
B) Count of Rods in 2 by 3 micron area from SEM images.

4.4 Effect of transition metal salts on the synthesis of silver nanorods:

Chloride salts of the transition metals manganese, iron and copper were also evaluated. Table 4.4 provides the measured diameter, length and the normalized number of rods obtained when these salts were used in the microwave assisted polyol process. $FeCl_3$ resulted in relatively short rods with a diameter of 57 nm and an AR on the order of 9. $CuCl_2$ resulted in similarly stubby rods with an AR on the order of 8 to 23 depending on concentration of the salt. In contrast $MnCl_2$ resulted in relatively small diameter rods with AR on the order of 160 – 260 and of the three transition metals evaluated seems the most suitable for the production of high aspect ratio Ag nanowires using the microwave assisted process. The use of MnCl2 results in rods with smaller diameters and longer lengths than NaCl at a similar yield. Figure 4.6 shows the SEM images of the MnCl2, CuCl2, and FeCl3 salts at 2.15 and 4.3mM concentrations.

There has been some work done on synthesis of silver nanowires using salts $FeCl_3$ and $CuCl_2$ in the traditional polyol synthesis of Ag nanorods. [141, 132] Both Wiley and Korte's work demonstrated that both the cation and anion play a role in the formation and growth of silver nanowires. The anion Cl^- acts as electrostatic stabilizer for the initially formed seeds and helps in controlled release of Ag^+ ions at the growth stage of silver nanoparticles. It has also been postulated to limit the availability of Ag^+ ions thereby controlling the overall reduction of Ag^+ to Ag^0 allowing directed growth to occur.

On the other hand high concentration of Cl^- ion leads to etching of twinned seeds. Two concentrations of salt were tested for those cations with a valance greater than one. For divalent and trivalent materials tests were performed with the ratio of Cl^- to Ag at very low ratios. In the case of Fe the Cl^- to Ag ratios tested were 1:6 and 1:2. As the data in table 4.4 indicates in every

case higher Cl^- concentrations resulted in fewer rods. In fact at higher of the two concentrations for $FeCl_3$ evaluated no rods were formed.

Table 4.4: Rod diameter, length, and # produced for transition metal salts evaluated.

	Concentration (nM)			Ag Rod / Wire Properties Mean and (Std. Dev.)			
Salt	**Metal**	**Chlorine**	**Cl:$AgNO_3$ Ratio**	**Diameter (nm)**	**Length (μm)**	**Nominal AR[a]**	**# of rods[b]**
$MnCl_2$	2.15	4.3	1:06	31.9 (8.6)	8.4 (1.8)	263	61 (9)
	4.3	8.6	1:03	41.8 (10.5)	7 (2.5)	167	29 (4)
$FeCl_3$	1.43	4.3	1:06	57.3 (23.2)	0.5 (0.3)	9	23 (8)
	4.3	12.9	1:02	52.5 (24.6)	NA		None
$CuCl_3$	2.15	4.3	1:06	118.8 (52.7)	2.7 (1.6)	23	13 (3)
	4.3	8.6	1:03	168.7 (48.4)	1.3 (0.7)	8	9 (1)

A) Based on mean length and diameter.
B) Count of Rods in 2 by 3 micron area from SEM images.

This might be due to higher concentration ratios of Cl^- to Ag in comparison to the previous work by both Wiley and Korte. Also conventional polyol method has been used in both the previous work. This indicates that different salts have different optimum concentration ratios of Cl^- to Ag to synthesis silver nanowires or any nanostructure.

The presence of disassociated O_2 on the seed surface blocks the further deposition of Ag, limiting seed growth. Korte et. al. limited this effect by adding cations with multiple valence states that are capable of scavenging oxygen from the growing silver surface. [132, 141] Both Fe^{2+} and Cu^{2+} have been demonstrated to affect the silver growth by scavenging oxygen facilitating the growth of nanorods.

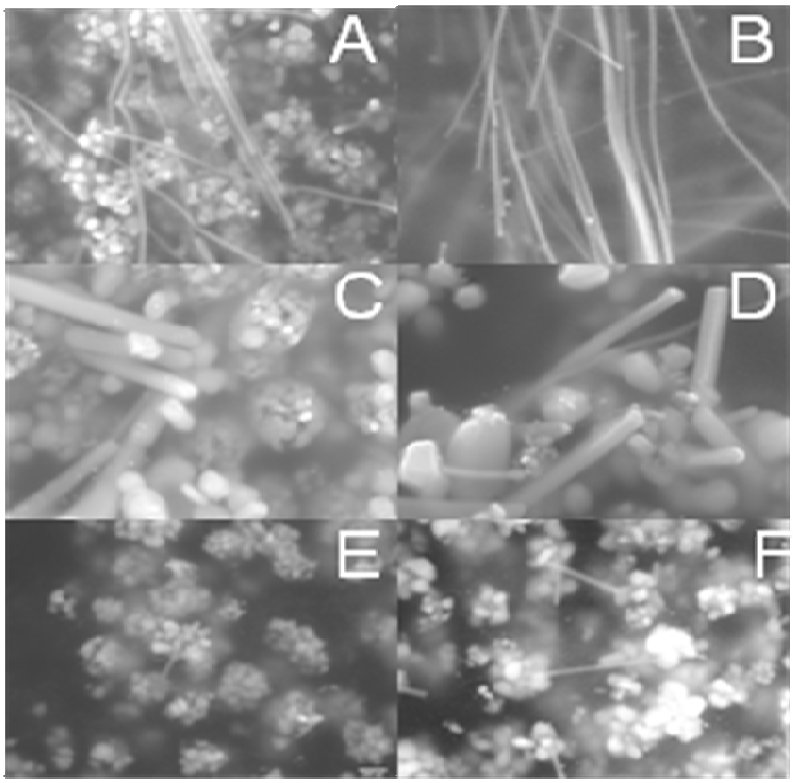

Figure 4.6: SEM images of silver nanorods using A) MnCl2, B) MnCl2, C) CuCl2, D) CuCl2, E) FeCl3 and F) FeCl3. A, C and E a 4.6mM and B, D and F at 2.15mM.

Table 4.5: Rod diameter, length, and # produced for effect of concentration of transition metal salt ($MnCl_2$) evaluated.

		Concentration (mM)			Ag Rod / Wire Properties Mean and (Std. Dev.)			
Salt	**Atomic Radius Metal (pm)**	**Metal**	**Chlorine**	**Cl:$AgNO_3$ Ratio**	**Diameter (nm)**	**Length (μm)**	**Nominal AR[a]**	**# of rods[b]**
$MnCl_2$	160	0.268	0.537	1:48	28.6 (5.9)	2.7 (0.8)	94.4	23 (12)
		0.537	1.075	1:24	38.1 (8.6)	7.9 (2.2)	207.3	46 (25)
		1.075	2.15	1:12	44.5 (12.5)	4.7 (1.5)	105.6	15 (2)
		2.15	4.3	1:06	31.9 (8.6)	8.4 (1.8)	263.3	61 (9)
		3.225	6.42	1:04	39.1 (8.4)	9.4 (3.7)	240.4	21 (2)
		4.3	8.6	1:03	41.8 (10.5)	7.1 (2.5)	169.8	29 (4)

A) Based on mean length and diameter.
B) Count of Rods in 2 by 3 micron area from SEM images.

In contrast to previous work we did not observe an increase in rod formation when using copper and ferric chlorides over the use of NaCl. The rods produced at all concentrations of $FeCl_3$ and $CuCl_2$ tested were large in diameter, shorter, and less in number. In previous studies the reaction was conducted over a period of several hours, while in the current study the reaction proceeds to completion in ~5 min. The much faster reaction times my not allow for the removal of O_2 from the growing rods surface limiting the growth.

To see the effect of concentration of salts, MnCl2 salt with total of 6 different concentrations were synthesized. Table 4.5 gives the details of the concentrations, diameter, length and number of rods. MnCl2 at 1.075mM gave the 80, highest number of rods compared to other concentrations. No pattern was followed in case of diameter, length and number of rods with respect to change in the concentration. Figure 4.7 shows the SEM images of silver nanoparticles at different concentrations.

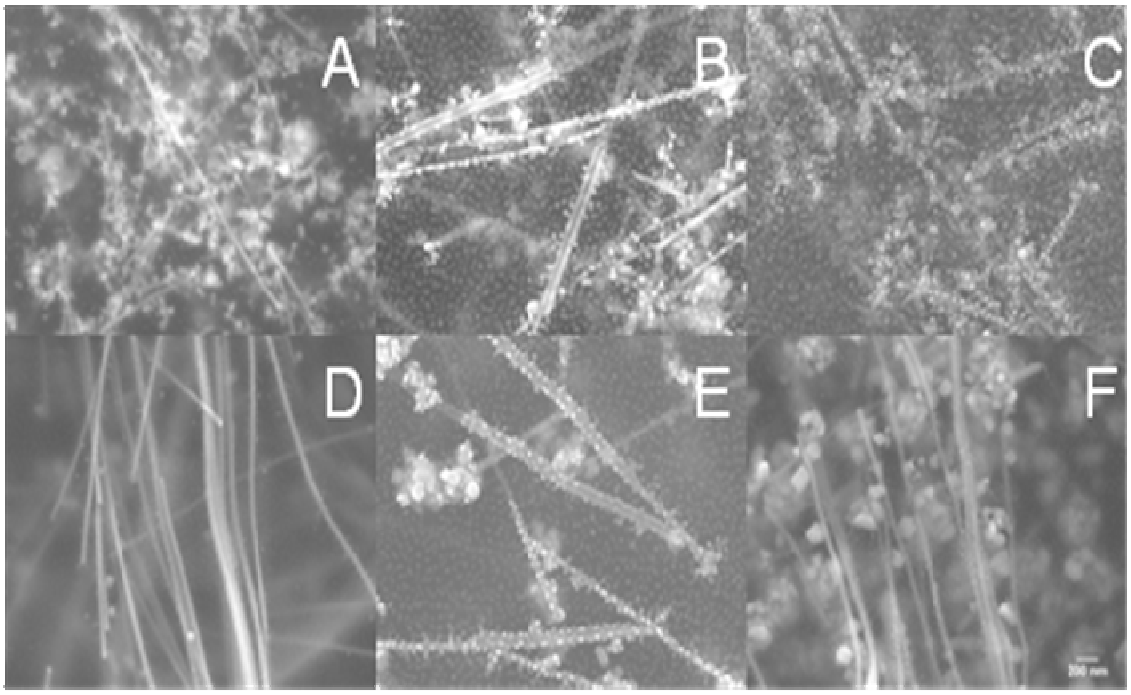

FIGURE 4.7: SEM images of silver nanoparticles using MnCl2 salt at A) 0.268mM, B) 0.537mM, C) 1.075mM, D) 2.15mM, E) 3.225mM, and F) 4.3mM

4.5 Effect of mixing methods on the synthesis of silver nanorods:

The Mixing method of stock solutions also has an impact on the final morphology of the final product. We have looked at 5 different mixing procedures as shown in the Table 4.6. All the methods used the same concentrations of PVP, $AgNO_3$ and KCl.

Table 4.6: Effect of mixing methods on final morphology

Method	Mixing method	mixing time (mins)	N_2 gas (mins)	Waiting time (mins)	Cl:$AgNO_3$	Dia (nm)	Length (µm)	Nominal AR[a]	No of rods[b]
I	Hand	Quick	1	0	1:06	35.5(6.4)	8.3(1.4)	234	40(12)
II	Hand	2	1	0	1:06	33.7(8.4)	10.1(2)	300	64(8)
III	Sonication	2	1	0	1:06	30.1(5.8)	7.3(1.6)	243	42(3)
IV	Hand	Quick	0	0	1:06	34.3(5.4)	8.6(2.7)	251	47(17)
V	Hand	Quick	1	10	1:06	42.3(17.3)	NA	NA	None

A) Based on mean length and diameter.
B) Count of Rods in 2 by 3 micron area from SEM images.

Figure 4.8 shows the SEM images of the silver nanoparticles synthesized using different mixing methods. Method II, Hand mixing for 2 minutes and purging with N_2 gas for 1 minute has given maximum number of rods with high AR of 300. Mixing through sonication (Method III) gave small diameter, short length and few rods when compared to hand mixing (Method II) under similar conditions. Hand mixing without N_2 gas purge (Method IV) did not made much difference compared to (Method I) hand mixing with N_2 gas purge. Interestingly, waiting for 10 minutes after mixing before microwave heating, Method V resulted in no nanorods. This might be due to the exposure of the solution to the atmospheric oxygen and moisture.

EG has the affinity to absorb the moisture from the atmosphere, where some of the microwave energy has been utilized to remove this moisture. In case of atmospheric oxygen, the presence of disassociated O_2 on the seed surface blocks the further deposition of Ag in {111} direction, limiting seed growth. [143]

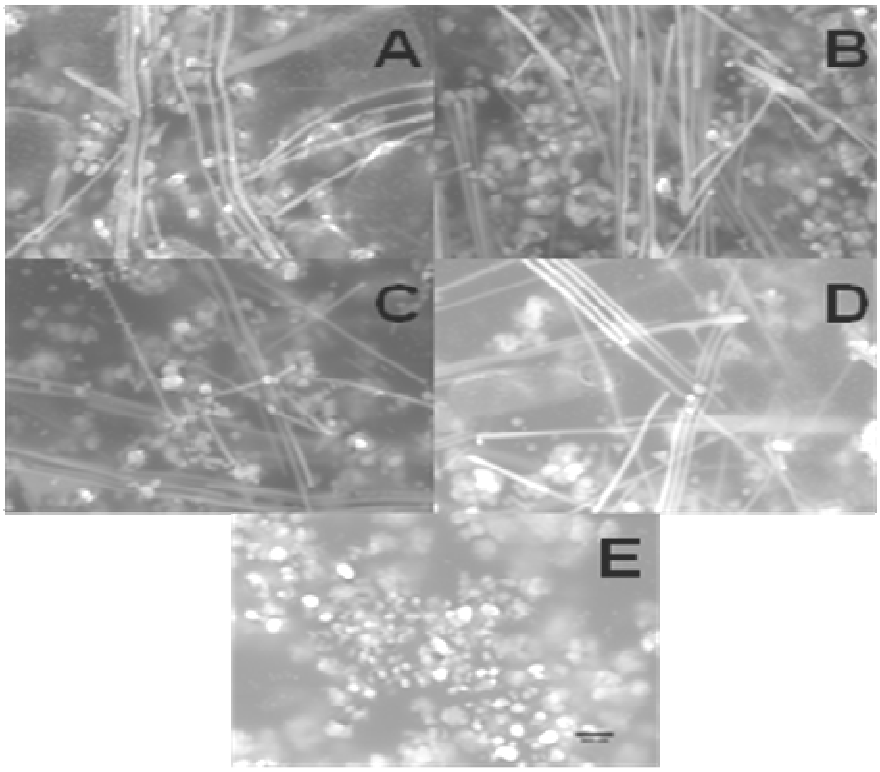

Figure 4.8: SEM images of silver nanoparticles synthesized using different mixing methods as shown in Table 2, A) Method I, B) Method II, C) Method III, D) Method IV, E) Method V.

Chapter 5

Conclusion

Synthesis and yield of silver nanorods is influenced by the shape of the container, where glass beaker with 5cm diameter gave high rods/spheres ratio. In the case of salts, the alkali and alkali earth metal salts have shown better results compared to transition metal salts. Salts like NaCl, KCl and MnCl2 at 4.3mM concentration gave good results for the synthesis of silver nanorods compared to other salts. Silver nanorods synthesis does have the effect of concentration of salt. Seems like each salt has its own optimum concentration, where the salt at that concentration gives maximum number of rods. Effect of mixing methods has shown a very interesting results, where waiting before applying microwave power has resulted in no nanorods. Continuous flow synthesis of silver nanorods resulted in nanospheres due to the accumulation of silver atoms on the glass tube. Modification of glass tube surface needs to be done in order to produce silver nanorods or any other structure.

References:

1. McFarland, A. D.; Van Duyne, R. P., Single Silver Nanoparticles as Real-Time Optical Sensors with Zeptomole Sensitivity. *Nano Letters* **2003,** *3* (8), 1057-1062.
2. Evanoff, D. D., Jr.; Chumanov, G., Synthesis and optical properties of silver nanoparticles and arrays. *ChemPhysChem* **2005,** *6* (7), 1221-1231.
3. Shanmukh, S.; Jones, L.; Driskell, J.; Zhao, Y.; Dluhy, R.; Tripp, R. A., Rapid and Sensitive Detection of Respiratory Virus Molecular Signatures Using a Silver Nanorod Array SERS Substrate. *Nano Letters* **2006,** *6* (11), 2630-2636.
4. Bernabo, M.; Pucci, A.; Ramanitra, H. H.; Ruggeri, G., Polymer nanocomposites containing anisotropic metal nanostructures as internal strain indicators. *Materials* **2010,** *3*, 1461-1477.
5. Hu, L.; Choi, J. W.; Yang, Y.; Jeong, S.; La Mantia, F.; Cui, L.-F.; Cui, Y., Highly conductive paper for energy-storage devices. *Proceedings of the National Academy of Sciences of the United States of America* **2009,** *106* (51), 21490-21494, S21490/1-S21490/13.
6. Darsey, J. A.; Buzatu, D. A., Computational nanotechnology: computational design and analysis of nanosize electronic components and circuits. *Handbook of Theoretical and Computational Nanotechnology* **2006,** *10*, 437-468.
7. Gogotsi, Y. G.; Uvarova, I. V., *Nanostructured materials and Coatings for Biomedical and Sensor Applications. (Proceedings of the NATO Advanced Research Workshop held in Kyiv, Ukraine 4-8 August 2002.) [In: NATO Sci. Ser., II, 2003; 102]*. 2003; p 397 pp.
8. Zhao, W.; Cao, H.; Wan, C.-s.; Zhang, W.-b., Application of nanotechnology in biomedical sciences. *Diyi Junyi Daxue Xuebao* **2002,** *22* (5), 461-463,465.
9. Schmid, G., Large clusters and colloids. Metals in the embryonic state. *Chem. Rev.* **1992,** *92* (8), 1709-27.
10. Daniel, M.-C.; Astruc, D., Gold Nanoparticles: Assembly, Supramolecular Chemistry, Quantum-Size-Related Properties, and Applications toward Biology, Catalysis, and Nanotechnology. *Chem. Rev. (Washington, DC, U. S.)* **2004,** *104* (1), 293-346.
11. Wong, T. S.; Schwaneberg, U., Protein engineering in bioelectrocatalysis. *Current Opinion in Biotechnology* **2003,** *14* (6), 590-596.
12. Ramanavicius, A.; Kausaite, A.; Ramanaviciene, A., Biofuel cell based on direct bioelectrocatalysis. *Biosensors & Bioelectronics* **2005,** *20* (10), 1962-1967.
13. Faraday, M., The Baker Lecture: Experimental of Gold (and other metals) to light. *Philosophical Transactions of Royal Society of London* **1857,** *147*, 147-181.
14. Cao, G., Nanostructures & Nanomaterials: Synthesis, Properties & Apllications. **2004**, 7-10.
15. Mie, G., Contributions to the Optics of Turbid Media, Especially Colloidal Metal Solutions. *Annalen der Physik (Weinheim, Germany)* **1908,** *25*, 377-445.

16. Kohra, K.; Kikuta, S., Theory and application of x-ray diffraction micrography. *Oyo Butsuri* **1967,** *36* (2), 88-104.
17. Murat, M., Scanning electron microscopy. Principles, apparatus, and use in solid and material chemistry. *Chimica e l'Industria (Milan, Italy)* **1975,** *57* (2), 99-113.
18. Pawley, J., The development of field-emission scanning electron microscopy for imaging biological surfaces. *Scanning* **1997,** *19* (5), 324-36.
19. Konno, M.; Yaguchi, T.; Hashimoto, T., Transmission electron microscope and scanning transmission electron microscope. *Shikizai Kyokaishi* **2006,** *79* (4), 147-151.
20. Ebert, P., Scanning probe microscopy: overview. *Schriften des Forschungszentrums Juelich, Reihe Materie und Material* **2007,** *34* (Probing the Nanoworld: Microscopies, Scattering and Spectroscopies of the Solid State), B4/1-B4/45.
21. Schneider, W. D., Scanning tunneling microscopy/spectroscopy of nanostructures. *Physica Status Solidi A: Applied Research* **2001,** *187* (1), 125-136.
22. Francis, L. W.; Lewis, P. D.; Wright, C. J.; Conlan, R. S., Atomic force microscopy comes of age. *Biology of the Cell* **2010,** *102* (2), 133-143.
23. Oikawa, T., Energy dispersive x-ray spectroscopy (EDS). *Toraiborojisuto* **2006,** *51* (2), 122-126.
24. Kang, H. J., Auger electron spectroscopy. *Hwahak Sekye* **2003,** *43* (12), 36-41.
25. Yoshida, Y., X-ray photoelectron spectroscopy (XPS). *Nippon Setchaku Gakkaishi* **2008,** *44* (5), 188-192.
26. Zhao, Y. S.; Fu, H.; Peng, A.; Ma, Y.; Xiao, D.; Yao, J., Low-dimensional nanomaterials based on small organic molecules: preparation and optoelectronic properties. *Advanced Materials (Weinheim, Germany)* **2008,** *20* (15), 2859-2876.
27. Peng, A.-D.; Xiao, D.-B.; Ma, Y.; Yang, W.-S.; Yao, J.-N., Tunable emission from doped 1,3,5-triphenyl-2-pyrazoline organic nanoparticles. *Advanced Materials (Weinheim, Germany)* **2005,** *17* (17), 2070-2073.
28. Zhao, Y. S.; Wu, J.; Huang, J., Vertical organic nanowire arrays: Controlled synthesis and chemical sensors. *Journal of the American Chemical Society* **2009,** *131* (9), 3158-3159.
29. An, B.-K.; Kwon, S.-K.; Jung, S.-D.; Park, S. Y., Enhanced emission and its switching in fluorescent organic nanoparticles. *Journal of the American Chemical Society* **2002,** *124* (48), 14410-14415.
30. An, B.-K.; Kwon, S.-K.; Park, S. Y., Photopatterned arrays of fluorescent organic nanoparticles. *Angewandte Chemie, International Edition* **2007,** *46* (12), 1978-1982.
31. Fu, H.-B.; Yao, J.-N., Size Effects on the Optical Properties of Organic Nanoparticles. *Journal of the American Chemical Society* **2001,** *123* (7), 1434-1439.
32. Debuigne, F.; Jeunieau, L.; Wiame, M.; Nagy, J. B., Synthesis of Organic Nanoparticles in Different W/O Microemulsions. *Langmuir* **2000,** *16* (20), 7605-7611.
33. Hu, S.-L.; Niu, K.-Y.; Sun, J.; Yang, J.; Zhao, N.-Q.; Du, X.-W., One-step synthesis of fluorescent carbon nanoparticles by laser irradiation. *Journal of Materials Chemistry* **2009,** *19* (4), 484-488.
34. Asahi, T.; Sugiyama, T.; Masuhara, H., Laser fabrication and spectroscopy of organic nanoparticles. *Acc Chem Res* **2008,** *41* (12), 1790-8.
35. Zhou, M.; Duan, X.; Ma, Y.; Zhou, Y.; Pei, C.; Luo, Q., Morphology control and optical properties of organic nanostructures based on thermotropic liquid crystalline benzoylated bacterial cellulose. *Carbohydrate Polymers* **2010,** *80* (2), 551-554.

36. Zhang, X.; Zhang, X.; Zou, K.; Lee, C.-S.; Lee, S.-T., Single-Crystal Nanoribbons, Nanotubes, and Nanowires from Intramolecular Charge-Transfer Organic Molecules. *Journal of the American Chemical Society* **2007,** *129* (12), 3527-3532.
37. Vriezema, D. M.; Hoogboom, J.; Velonia, K.; Takazawa, K.; Christianen, P. C. M.; Maan, J. C.; Rowan, A. E.; Nolte, R. J. M., Vesicles and polymerized vesicles from thiophene-containing rod-coil block copolymers. *Angewandte Chemie, International Edition* **2003,** *42* (7), 772-776.
38. Balakrishnan, K.; Datar, A.; Naddo, T.; Huang, J.; Oitker, R.; Yen, M.; Zhao, J.; Zang, L., Effect of Side-Chain Substituents on Self-Assembly of Perylene Diimide Molecules: Morphology Control. *Journal of the American Chemical Society* **2006,** *128* (22), 7390-7398.
39. Zhao Yong, S.; Fu, H.; Peng, A.; Ma, Y.; Liao, Q.; Yao, J., Construction and optoelectronic properties of organic one-dimensional nanostructures. *Acc Chem Res* **2010,** *43* (3), 409-18.
40. Zang, L.; Che, Y.; Moore, J. S., One-Dimensional Self-Assembly of Planar pi-Conjugated Molecules: Adaptable Building Blocks for Organic Nanodevices. *Accounts of Chemical Research* **2008,** *41* (12), 1596-1608.
41. Fardy, M.; Yang, P., Lilliputian light sticks. *Nature (London, United Kingdom)* **2008,** *451* (7177), 408-409.
42. Zhao, Y. S.; Fu, H.; Hu, F.; Peng, A.; Yang, W.; Yao, J., Tunable emission from binary organic one-dimensional nanomaterials: an alternative approach to white-light emission. *Advanced Materials (Weinheim, Germany)* **2008,** *20* (1), 79-83.
43. Briseno, A. L.; Mannsfeld, S. C. B.; Lu, X.; Xiong, Y.; Jenekhe, S. A.; Bao, Z.; Xia, Y., Fabrication of Field-Effect Transistors from Hexathiapentacene Single-Crystal Nanowires. *Nano Letters* **2007,** *7* (3), 668-675.
44. Che, Y.; Yang, X.; Loser, S.; Zang, L., Expedient vapor probing of organic amines using fluorescent nanofibers fabricated from an n-type organic semiconductor. *Nano Letters* **2008,** *8* (8), 2219-2223.
45. O'Carroll, D.; Lieberwirth, I.; Redmond, G., Microcavity effects and optically pumped lasing in single conjugated polymer nanowires. *Nature Nanotechnology* **2007,** *2* (3), 180-184.
46. Iijima, S., Helical microtubules of graphitic carbon. *Nature (London)* **1991,** *354* (6348), 56-8.
47. Guo, T.; Nikolaev, P.; Thess, A.; Colbert, D. T.; Smalley, R. E., Catalytic growth of single-walled nanotubes by laser vaporization. *Chemical Physics Letters* **1995,** *243* (1,2), 49-54.
48. Shen, G. Z.; Chen, D.; Tang, K. B.; Qian, Y. T.; Lee, C. J., High-yield solvo-thermal synthesis of carbon nanotubes from sp3 hydrocarbons. *Applied Physics A: Materials Science & Processing* **2005,** *81* (3), 523-526.
49. Nikolaev, P.; Bronikowski, M. J.; Bradley, R. K.; Rohmund, F.; Colbert, D. T.; Smith, K. A.; Smalley, R. E., Gas-phase catalytic growth of single-walled carbon nanotubes from carbon monoxide. *Chemical Physics Letters* **1999,** *313* (1,2), 91-97.
50. Dervishi, E.; Li, Z.; Xu, Y.; Saini, V.; Biris, A. R.; Lupu, D.; Biris, A. S., Carbon nanotubes: synthesis, properties, and applications. *Particulate Science and Technology* **2009,** *27* (2), 107-125.
51. Kataura, H.; Kumazawa, Y.; Maniwa, Y.; Umezu, I.; Suzuki, S.; Ohtsuka, Y.; Achiba, Y., Optical properties of single-wall carbon nanotubes. *Synthetic Metals* **1999,** *103* (1-3), 2555-2558.
52. Pang, W.-q.; Fan, X.-z., Application progress of nanometer metal oxide catalysts in solid propellant. *Huaxue Tuijinji Yu Gaofenzi Cailiao* **2008,** *6* (2), 16-20.

53. Poizot, P.; Laruelle, S.; Grugeon, S.; Dupont, L.; Tarascon, J. M., Nano-sized transition-metal oxides as negative-electrode materials for lithium-ion batteries. *Nature* **2000,** *407* (6803), 496-9.
54. Shigehito D.; Akiyoshi N.; M., M., Nanostructured Metal Oxides: Processing and Applications. **2006,** (9), 29-35.
55. Niederberger, M., Nonaqueous Sol-Gel Routes to Metal Oxide Nanoparticles. *Accounts of Chemical Research* **2007,** *40* (9), 793-800.
56. Reuge, N.; Bacsa, R.; Serp, P.; Caussat, B., Chemical Vapor Synthesis of Zinc Oxide Nanoparticles: Experimental and Preliminary Modeling Studies. *Journal of Physical Chemistry C* **2009,** *113* (46), 19845-19852.
57. Lisiecki, I.; Pileni, M. P., Synthesis of copper metallic clusters using reverse micelles as microreactors. *Journal of the American Chemical Society* **1993,** *115* (10), 3887-96.
58. Han, D. Y.; Yang, H. Y.; Shen, C. B.; Zhou, X.; Wang, F. H., Synthesis and size control of NiO nanoparticles by water-in-oil microemulsion. *Powder Technology* **2004,** *147* (1-3), 113-116.
59. Kim, M. H.; Lim, B.; Lee, E. P.; Xia, Y., Polyol synthesis of Cu2O nanoparticles: use of chloride to promote the formation of a cubic morphology. *Journal of Materials Chemistry* **2008,** *18* (34), 4069-4073.
60. H. Zhao; Ning, Y., Techniques Used for the Preparation and Application of Gold Powder in Ancient China. *Gold Bulletin* **2000,** *33* (3), 103-105.
61. Camusso, L., Ceramics of the World: From 4000 B. C. to the Present. **1992**, 284.
62. J. Turkevich; P. C. Stevenson; Hiller, J., *Disc. Faraday Soc.* **1951,** *11*, 55-75.
63. Lee, P. C.; Meisel, D., Adsorption and surface-enhanced Raman of dyes on silver and gold sols. *Journal of Physical Chemistry* **1982,** *86* (17), 3391-5.
64. Creighton, J. A.; Blatchford, C. G.; Albrecht, M. G., Plasma resonance enhancement of Raman scattering by pyridine adsorbed on silver or gold sol particles of size comparable to the excitation wavelength. *Journal of the Chemical Society, Faraday Transactions 2: Molecular and Chemical Physics* **1979,** *75* (5), 790-8.
65. Ayyappan, S.; Srinivasa Gopalan, R.; Subbanna, G. N.; Rao, C. N. R., Nanoparticles of Ag, Au, Pd, and Cu produced by alcohol reduction of the salts. *Journal of Materials Research* **1997,** *12* (2), 398-401.
66. Longenberger, L.; Mills, G., Formation of Metal Particles in Aqueous Solutions by Reactions of Metal Complexes with Polymers. *Journal of Physical Chemistry* **1995,** *99* (2), 475-8.
67. Sastry, M.; Patil, V.; Mayya, K. S.; Paranjape, D. V.; Singh, P.; Sainkar, S. R., Organization of polymer-capped platinum colloidal particles at the air-water interface. *Thin Solid Films* **1998,** *324* (1,2), 239-244.
68. Scott, R. W. J.; Ye, H.; Henriquez, R. R.; Crooks, R. M., Synthesis, Characterization, and Stability of Dendrimer-Encapsulated Palladium Nanoparticles. *Chemistry of Materials* **2003,** *15* (20), 3873-3878.
69. Sinha, A.; Das, S. K.; Kumar, T. V. V.; Rao, V.; Ramachandrarao, P., Synthesis of nanosized copper powder by an aqueous route. *Journal of Materials Synthesis and Processing* **1999,** *7* (6), 373-377.
70. Hou, Y.; Gao, S., Monodisperse nickel nanoparticles prepared from a monosurfactant system and their magnetic properties. *Journal of Materials Chemistry* **2003,** *13* (7), 1510-1512.

71. Narayanan, K. B.; Sakthivel, N., Biological synthesis of metal nanoparticles by microbes. *Advances in Colloid and Interface Science* **2010,** *156* (1-2), 1-13.
72. Cook, S. C.; Padmos, J. D.; Zhang, P., Surface structural characteristics and tunable electronic properties of wet-chemically prepared Pd nanoparticles. *Journal of Chemical Physics* **2008,** *128* (15), 154705/1-154705/11.
73. Hotchkiss, J. W.; Mohr, B. G. R.; Boyes, S. G., Gold nanorods surface modified with poly(acrylic acid) as a template for the synthesis of metallic nanoparticles. *Journal of Nanoparticle Research* **2010,** *12* (3), 915-930.
74. Viau, G.; Fievet-Vincent, F.; Fievet, F., Nucleation and growth of bimetallic CoNi and FeNi monodisperse particles prepared in polyols. *Solid State Ionics* **1996,** *84* (3,4), 259-270.
75. Yang, H.; Shen, C.; Gao, H., Solution-phase synthesis of metal nanoparticles. *Wuli* **2003,** *32* (8), 520-527.
76. Fujimoto, T.; Terauchi, S.-y.; Umehara, H.; Kojima, I.; Henderson, W., Sonochemical Preparation of Single-Dispersion Metal Nanoparticles from Metal Salts. *Chemistry of Materials* **2001,** *13* (3), 1057-1060.
77. Ulan, J. G.; Maier, W. F.; Smith, D. A., Rational design of a heterogeneous palladium catalyst for the selective hydrogenation of alkynes. *Journal of Organic Chemistry* **1987,** *52* (14), 3132-42.
78. Narayanan, R.; El-Sayed, M. A., Shape-Dependent Catalytic Activity of Platinum Nanoparticles in Colloidal Solution. *Nano Letters* **2004,** *4* (7), 1343-1348.
79. Kolmakov, A.; Klenov, D. O.; Lilach, Y.; Stemmer, S.; Moskovits, M., Enhanced gas sensing by individual SnO2 nanowires and nanobelts functionalized with Pd catalyst particles. *Nano Letters* **2005,** *5* (4), 667-673.
80. Xia, Y.; Halas, N. J., Shape-controlled synthesis and surface plasmonic properties of metallic nanostructures. *MRS Bulletin* **2005,** *30* (5), 338-348.
81. Sondi, I.; Goia, D. V.; Matijevic, E., Preparation of highly concentrated stable dispersions of uniform silver nanoparticles. *Journal of Colloid and Interface Science* **2003,** *260* (1), 75-81.
82. Chen, D.-H.; Huang, Y.-W., Spontaneous formation of Ag nanoparticles in dimethylacetamide solution of poly(ethylene glycol). *Journal of Colloid and Interface Science* **2002,** *255* (2), 299-302.
83. Li, X.; Zhang, J.; Xu, W.; Jia, H.; Wang, X.; Yang, B.; Zhao, B.; Li, B.; Ozaki, Y., Mercaptoacetic Acid-Capped Silver Nanoparticles Colloid: Formation, Morphology, and SERS Activity. *Langmuir* **2003,** *19* (10), 4285-4290.
84. Shirtcliffe, N.; Nickel, U.; Schneider, S., Reproducible preparation of silver sols with small particle size using borohydride reduction: for use as nuclei for preparation of larger particles. *Journal of Colloid and Interface Science* **1999,** *211* (1), 122-129.
85. He, S.; Yao, J.; Jiang, P.; Shi, D.; Zhang, H.; Xie, S.; Pang, S.; Gao, H., Formation of silver nanoparticles and self-assembled two-dimensional ordered superlattice. *Langmuir* **2001,** *17* (5), 1571-1575.
86. Nickel, U.; zu Castell, A.; Poeppl, K.; Schneider, S., A silver colloid produced by reduction with hydrazine as support for highly sensitive surface-enhanced Raman spectroscopy. *Langmuir* **2000,** *16* (23), 9087-9091.
87. He, R.; Qian, X.; Yin, J.; Zhu, Z., Preparation of polychrome silver nanoparticles in different solvents. *Journal of Materials Chemistry* **2002,** *12* (12), 3783-3786.
88. Van Hyning, D. L.; Zukoski, C. F., Formation Mechanisms and Aggregation Behavior of Borohydride Reduced Silver Particles. *Langmuir* **1998,** *14* (24), 7034-7046.

89. Li, G.-P.; Luo, Y.-J.; Tan, H.-M., Preparation of silver nanoparticles using dendrimer as template. *Huaxue Xuebao* **2004,** *62* (12), 1158-1161.
90. Parikh, R. Y.; Singh, S.; Prasad, B. L. V.; Patole, M. S.; Sastry, M.; Shouche, Y. S., Extracellular synthesis of crystalline silver nanoparticles and molecular evidence of silver resistance from Morganella sp.: towards understanding biochemical synthesis mechanism. *ChemBioChem* **2008,** *9* (9), 1415-1422.
91. Yu, D.; Sun, X.; Bian, J.; Tong, Z.; Qian, Y., Gamma-radiation synthesis, characterization and nonlinear optical properties of highly stable colloidal silver nanoparticles in suspensions. *Physica E: Low-Dimensional Systems & Nanostructures (Amsterdam, Netherlands)* **2004,** *23* (1-2), 50-55.
92. Pyatenko, A.; Shimokawa, K.; Yamaguchi, M.; Nishimura, O.; Suzuki, M., Synthesis of silver nanoparticles by laser ablation in pure water. *Applied Physics A: Materials Science & Processing* **2004,** *79* (4-6), 803-806.
93. Rosemary, M. J.; Pradeep, T., Solvothermal synthesis of silver nanoparticles from thiolates. *J Colloid Interface Sci* **2003,** *268* (1), 81-4.
94. Khaydarov, R. A.; Khaydarov, R. R.; Gapurova, O.; Estrin, Y.; Scheper, T., Electrochemical method for the synthesis of silver nanoparticles. *Journal of Nanoparticle Research* **2009,** *11* (5), 1193-1200.
95. Donati, I.; Travan, A.; Pelillo, C.; Scarpa, T.; Coslovi, A.; Bonifacio, A.; Sergo, V.; Paoletti, S., Polyol synthesis of silver nanoparticles: mechanism of reduction by alditol bearing polysaccharides. *Biomacromolecules* **2009,** *10* (2), 210-3.
96. Tien, D.-C.; Tseng, K.-H.; Liao, C.-Y.; Tsung, T.-T., Colloidal silver fabrication using the spark discharge system and its antimicrobial effect on Staphylococcus aureus. *Medical engineering & physics* **2008,** *30* (8), 948-52.
97. Sahoo, P. K.; Kamal, S. S. K.; Kumar, T. J.; Sreedhar, B.; Singh, A. K.; Srivastava, S. K., Synthesis of silver nanoparticles using facile wet chemical route. *Defence Science Journal* **2009,** *59* (4), 447-455.
98. Yang, G.-W.; Li, H., Sonochemical synthesis of highly monodispersed and size controllable Ag nanoparticles in ethanol solution. *Materials Letters* **2008,** *62* (14), 2193-2195.
99. Maretti, L.; Billone, P. S.; Liu, Y.; Scaiano, J. C., Facile photochemical synthesis and characterization of highly fluorescent silver nanoparticles. *Journal of the American Chemical Society* **2009,** *131* (39), 13972-13980.
100. Fievet, F.; Lagier, J. P.; Blin, B.; Beaudoin, B.; Figlarz, M., Homogeneous and heterogeneous nucleations in the polyol process for the preparation of micron and submicron size metal particles. *Solid State Ionics* **1989,** *32-33* (Pt. I), 198-205.
101. Tsuji, M.; Hashimoto, M.; Nishizawa, Y.; Tsuji, T., Synthesis of gold nanorods and nanowires by a microwave-polyol method. *Materials Letters* **2004,** *58* (17-18), 2326-2330.
102. Park Bong, K.; Jeong, S.; Kim, D.; Moon, J.; Lim, S.; Kim Jang, S., Synthesis and size control of monodisperse copper nanoparticles by polyol method. *J Colloid Interface Sci* **2007,** *311* (2), 417-24.
103. Joseyphus, R. J.; Matsumoto, T.; Takahashi, H.; Kodama, D.; Tohji, K.; Jeyadevan, B., Designed synthesis of cobalt and its alloys by polyol process. *Journal of Solid State Chemistry* **2007,** *180* (11), 3008-3018.
104. Toneguzzo, P.; Viau, G.; Acher, O.; Fievet-Vincent, F.; Fievet, F., Monodisperse ferromagnetic particles for microwave applications. *Advanced Materials (Weinheim, Germany)* **1998,** *10* (13), 1032-1035.

105. Xiong, Y.; Chen, J.; Wiley, B.; Xia, Y.; Aloni, S.; Yin, Y., Understanding the role of oxidative etching in the polyol synthesis of Pd nanoparticles with uniform shape and size. *J Am Chem Soc* **2005,** *127* (20), 7332-3.
106. Herricks, T.; Chen, J.; Xia, Y., Polyol Synthesis of Platinum Nanoparticles: Control of Morphology with Sodium Nitrate. *Nano Letters* **2004,** *4* (12), 2367-2371.
107. Harpeness, R.; Peng, Z.; Liu, X.; Pol Vilas, G.; Koltypin, Y.; Gedanken, A., Controlling the agglomeration of anisotropic Ru nanoparticles by the microwave-polyol process. *J Colloid Interface Sci* **2005,** *287* (2), 678-84.
108. Wiley, B.; Sun, Y.; Xia, Y., Synthesis of Silver Nanostructures with Controlled Shapes and Properties. *Accounts of Chemical Research* **2007,** *40* (10), 1067-1076.
109. Sun, Y.; Mayers, B.; Xia, Y., Transformation of Silver Nanospheres into Nanobelts and Triangular Nanoplates through a Thermal Process. *Nano Letters* **2003,** *3* (5), 675-679.
110. Hoppe, C. E.; Lazzari, M.; Pardinas-Blanco, I.; Lopez-Quintela, M. A., One-Step Synthesis of Gold and Silver Hydrosols Using Poly(N-vinyl-2-pyrrolidone) as a Reducing Agent. *Langmuir* **2006,** *22* (16), 7027-7034.
111. Silvert, P.-Y.; Herrera-Urbina, R.; Duvauchelle, N.; Vijayakrishnan, V.; Elhsissen, K. T., Preparation of colloidal silver dispersions by the polyol process. Part 1. Synthesis and characterization. *Journal of Materials Chemistry* **1996,** *6* (4), 573-7.
112. Pastoriza-Santos, I.; Liz-Marzan, L. M., Formation of PVP-Protected Metal Nanoparticles in DMF. *Langmuir* **2002,** *18* (7), 2888-2894.
113. Carotenuto, G., Synthesis and characterization of poly(N-vinylpyrrolidone) filled by monodispersed silver clusters with controlled size. *Applied Organometallic Chemistry* **2001,** *15* (5), 344-351.
114. Sun, Y.; Xia, Y., Large-scale synthesis of uniform silver nanowires through a soft, self-seeding, polyol process. *Advanced Materials (Weinheim, Germany)* **2002,** *14* (11), 833-837.
115. B. Yin; H. Ma; S. Wang; Chen, S., Electrochemical synthesis of silver nanoparticles under protection of PVP. *Journal of Physical Chemistry B* **2003,** *107*, 8898-8904.
116. http://www.diytrade.com/china/4/products/1362842/Crosslinked_Polyvinylpyrrolidone_PVPP.html.
117. Sun, X.; Li, Y., Cylindrical silver nanowires: Preparation, structure, and optical properties. *Advanced Materials (Weinheim, Germany)* **2005,** *17* (21), 2626-2630.
118. Hu, L.; Kim, H. S.; Lee, J.-Y.; Peumans, P.; Cui, Y., Scalable coating and properties of transparent, flexible, silver nanowire electrodes. *ACS Nano* **2010,** *4* (5), 2955-2963.
119. Xu, X. J.; Fei, G. T.; Yu, W. H.; Zhang, L. D.; Ju, X.; Hao, X. P.; Wang, D. N.; Wang, B. Y., In situ x-ray diffraction study of the size dependent thermal expansion of silver nanowires. *Applied Physics Letters* **2006,** *89* (18), 181914/1-181914/3.
120. Tao, A.; Kim, F.; Hess, C.; Goldberger, J.; He, R.; Sun, Y.; Xia, Y.; Yang, P., Langmuir-Blodgett silver nanowire monolayers for molecular sensing using surface-enhanced Raman spectroscopy. *Nano Letters* **2003,** *3* (9), 1229-1233.
121. Kostowskyj, M. A.; Gilliam, R. J.; Kirk, D. W.; Thorpe, S. J., Silver nanowire catalysts for alkaline fuel cells. *International Journal of Hydrogen Energy* **2008,** *33* (20), 5773-5778.
122. Hu, X.; Chan, C. T., Photonic crystals with silver nanowires as a near-infrared superlens. *Applied Physics Letters* **2004,** *85* (9), 1520-1522.

123. Shtykov, S. N.; Rusanova, T. Y., Nanomaterials and nanotechnologies in chemical and biochemical sensors: Capabilities and applications. *Russian Journal of General Chemistry* **2008,** *78* (12), 2521-2531.
124. Hu, Z. A.; Xu, T.; Liu, R. J.; Li, H. L., Template preparation of high-density, and large-area Ag nanowire array by acetaldehyde reduction. *Materials Science & Engineering, A: Structural Materials: Properties, Microstructure and Processing* **2004,** *A371* (1-2), 236-240.
125. Caswell, K. K.; Bender, C. M.; Murphy, C. J., Seedless, Surfactantless Wet Chemical Synthesis of Silver Nanowires. *Nano Letters* **2003,** *3* (5), 667-669.
126. Yang, Y.; Matsubara, S.; Xiong, L.; Hayakawa, T.; Nogami, M., Solvothermal Synthesis of Multiple Shapes of Silver Nanoparticles and Their SERS Properties. *Journal of Physical Chemistry C* **2007,** *111* (26), 9095-9104.
127. Tsuji, M.; Matsumoto, K.; Miyamae, N.; Tsuji, T.; Zhang, X., Rapid Preparation of Silver Nanorods and Nanowires by a Microwave-Polyol Method in the Presence of Pt Catalyst and Polyvinylpyrrolidone. *Crystal Growth & Design* **2007,** *7* (2), 311-320.
128. Gou, L.; Chipara, M.; Zaleski, J. M., Convenient, rapid synthesis of Ag nanowires. *Chemistry of Materials* **2007,** *19* (7), 1755-1760.
129. Komarneni, S.; Li, Q. H.; Roy, R., Microwave-hydrothermal processing for synthesis of layered and network phosphates. *Journal of Materials Chemistry* **1994,** *4* (12), 1903-6.
130. Katsuki, H.; Komarneni, S., Microwave-hydrothermal synthesis of monodispersed nanophase alpha -Fe2O3. *Journal of the American Ceramic Society* **2001,** *84* (10), 2313-2317.
131. Chen, C.; Wang, L.; Jiang, G.; Zhou, J.; Chen, X.; Yu, H.; Yang, Q., Study on the synthesis of silver nanowires with adjustable diameters through the polyol process. *Nanotechnology* **2006,** *17* (15), 3933-3938.
132. Korte, K. E.; Skrabalak, S. E.; Xia, Y., Rapid synthesis of silver nanowires through a CuCl- or CuCl2-mediated polyol process. *Journal of Materials Chemistry* **2008,** *18* (4), 437-441.
133. Chan, E. M.; Mathies, R. A.; Alivisatos, A. P., Size-controlled growth of CdSe nanocrystals in microfluidic reactors. *Nano Letters* **2003,** *3* (2), 199-201.
134. Wang, H.; Nakamura, H.; Uehara, M.; Miyazaki, M.; Maeda, H., Preparation of titania particles utilizing the insoluble phase interface in a microchannel reactor. *Chemical Communications (Cambridge, United Kingdom)* **2002,** (14), 1462-1463.
135. Wagner, J.; Koehler, J. M., Continuous Synthesis of Gold Nanoparticles in a Microreactor. *Nano Letters* **2005,** *5* (4), 685-691.
136. Lin, X. Z.; Terepka, A. D.; Yang, H., Synthesis of Silver Nanoparticles in a Continuous Flow Tubular Microreactor. *Nano Letters* **2004,** *4* (11), 2227-2232.
137. Kohler, J. M.; Wager, J.; Albert, J., Formation of isolated and clustered Au nanoparticles in the presence of polyelectrolyte molecules using a flow-through Si chip reactor. *Journal of Materials Chemistry* **2005,** *15*, 1924-1930.
138. Clifford Y. Tai; Yao-Hsuan Wang; Chaia-Te Tai; Liu, H.-S., Preparation of Silver Nanoparticles Using a Spinning Disk Reactor in a Continuous Mode. *Ind. Eng. Chem. Res.* **2009,** *48*, 10104- 10109.
139. Chen, D.; Qiao, X.; Qiu, X.; Chen, J.; Jiang, R., Convenient, rapid synthesis of silver nanocubes and nanowires via a microwave-assisted polyol method. *Nanotechnology* **2010,** *21* (2), 025607/1-025607/7.
140. Wiley, B.; Sun, Y.; Mayers, B.; Xia, Y., Shape-controlled synthesis of metal nanostructures: The case of silver. *Chemistry--A European Journal* **2005,** *11* (2), 454-463.

141. Wiley, B.; Sun, Y.; Xia, Y., Polyol synthesis of silver nanostructures: control of product morphology with Fe(II) or Fe(III) species. *Langmuir* **2005,** *21* (18), 8077-8080.
142. Chen, D.; Qiao, X.; Qiu, X.; Chen, J.; Jiang, R., Convenient synthesis of silver nanowires with adjustable diameters via a solvothermal method. *Journal of Colloid and Interface Science* **2010,** *344* (2), 286-291.
143. Buatier de Mongeot, F.; Valbusa, U.; Rocca, M., Oxygen adsorption on Ag(111). *Surface Science* **1995,** *339* (3), 291-6.